# Optical Properties of $Cs_2TiBr_6$, a New Solar Energy Material

A Major Qualifying Project
submitted to the Faculty of
WORCESTER POLYTECHNIC INSTITUTE
in partial fulfillment of the requirements for the
degree of Bachelor of Science
in physics and the degree of Bachelor of Arts
in environmental and sustainability studies

by
Maranda Allen
Caroline Jaeger

Date:
March 25, 2022

Report Submitted to:

Professors Lyubov Titova, Robert Krueger, and Ronald Grimm
Worcester Polytechnic Institute

This report represents the work of WPI undergraduate students submitted to the faculty as evidence of a degree requirement. WPI routinely publishes these reports on its web site without editorial or peer review. For more information about the projects program at WPI, see http://www.wpi.edu/Academics/Projects.

# Abstract

The goal of this project was to use time-resolved photoluminescence spectroscopy to investigate optical emission and carrier lifetime in single crystal and thin film cesium titanium (IV) bromide $Cs_2TiBr_6$. $Cs_2TiBr_6$ is an all-inorganic lead-free halide perovskite-like material that shows promise for photovoltaic (PV) applications. This research is necessary to find non-toxic, inexpensive alternatives to current PV materials. We find that its optical properties demonstrate high stability in $N_2$ atmosphere, with photoexcited radiative lifetimes on the order of 0.5 ns, sufficient for photovoltaic consideration. We investigated the origins of several prominent emission features and their dependence on sample morphology and environmental conditions. We find that single crystal samples exhibit less homogeneity in emission and decay characteristics than their thin film counterparts. We also researched the sustainability of the material's extraction and usage, indicating the need for future acknowledgment of sourcing and safety concerns.

# Acknowledgements

We would like to thank our advisors on this project, Professors Titova, Krueger, and Grimm, for their continued support on this project. Professor Titova provided us with this project opportunity and served as an invaluable mentor in understanding photoluminescence spectroscopy and the interpretation of our data. Professor Krueger guided us in our research of the sustainability of the material, opening our eyes to unforeseen implications and allowing us to delve deeper into the unforeseen global implications of green technology. Professor Grimm, Julia Martin, and Emma Pellerin have been instrumental to our project by providing us with our material samples and giving us deeper insight into understanding the data obtained through our research. We also would like to thank Erika Colin Ulloa for her support throughout the project, mentoring us in using and setting up the photoluminescence spectroscopy equipment, data collection, and analysis programs.

# Authorship

Both authors contributed equally to the writing and editing of the abstract, executive summary, general background, methodology, results, discussion, and conclusion sections. Information about synthesis of samples (Appendix A) was provided by Emma Pellerin, a member of Grimmgroup in the Department of Chemistry and Biochemistry. The sustainability background chapter was written by Caroline Jaeger.

# Table of Contents

# Table of Figures

# Introduction

This project used time-resolved photoluminescence spectroscopy (PL) to investigate the optical emission and carrier lifetime in single crystal and thin-film $Cs_2TiBr_6$ samples, which have the potential to be used as a non-toxic, less expensive alternative for solar cells (Ju et al., 2018; Chen, et al. 2018)

The use of solar panels has increased in popularity as more effort has been directed towards renewable energy generation and reduction of fossil fuel emissions. Unfortunately, many of these renewable options involve harmful heavy metals such as lead (Pb). This has led to an increased amount of research into less toxic, Pb-free perovskite-based alternatives. A variety of alternative solar cell materials are being researched for the possibility of industrialization and exhibit a range of efficiencies. Over the past two decades, perovskite solar cells have experienced rapid increases to their PCEs. However, most perovskites being studied are lead-based and therefore still pose concerns related to toxicity. Thus, we have been looking into the efficiency potential of a Ti-based, completely inorganic perovskite-like material that eliminates the use of volatile organic ions and introduces a less toxic metal base. PVs made from this material have favorable band gaps in the visible range, long (>100 nm) diffusion lengths of photoexcited carriers and energy level structure that is suitable for PV applications (Chen et al., 2018, Euvrard et al., 2020). Titanium, the metal used as a replacement for lead and tin, is earth-abundant, inorganic, and nontoxic (Chen et al., 2018). Despite these positive developments, researchers' key concerns currently involve $Cs_2TiBr_6$'s low PCE and degradation under ambient environmental conditions (Correa-Baena et al., 2017; Mendes et al., 2020). There are also sourcing issues that deal with human rights violations and use of environmentally scarce materials, disrupting livelihoods and damaging local environments. These implications must be acknowledged before widespread implementation of the new technology can occur.

Herein, we investigated several single-crystal and thin-film samples sealed in a dry $N_2$ environment to prevent degradation. We used spectrally- and time-resolved PL measurements to determine the energy structure, excitation states, and radiative lifetimes of photoexcited carriers of the $Cs_2TiBr_6$ crystals and films. We discuss the results in the context of the viability of $Cs_2TiBr_6$ for solar-energy-conversion applications.

# I. Background

With an increasing emphasis on reduction of fossil fuel emissions and shifting towards renewable energy generation, solar panels are increasing in popularity and usage throughout the world and being looked to as a possible technological solution for energy production. Green energy sounds like an ideal substitute, but as with all material and technological substitution, it comes at a cost to both the environment and public health. These sources of renewable energy involve resources such as copper, lithium, cobalt, and other harmful heavy metals, thus leading to research into less toxic perovskite-based alternatives.

## 1. Existing Solar Cell Materials

There are currently a variety of different solar cell materials being researched for possible widespread implementation and industrialization. These include crystalline silicon cells, various thin film technologies, and emerging perovskite-based cells (Office of Energy Efficiency and Renewable Energy, n.d.). These materials exhibit a variety of different efficiencies, and newer technologies such as perovskite solar cells have experienced rapid improvements in PCEs over the past two decades (Office of Energy Efficiency and Renewable Energy, n.d.). Figure 1 displays the relative cell efficiencies of the various types of solar panels since 2000.

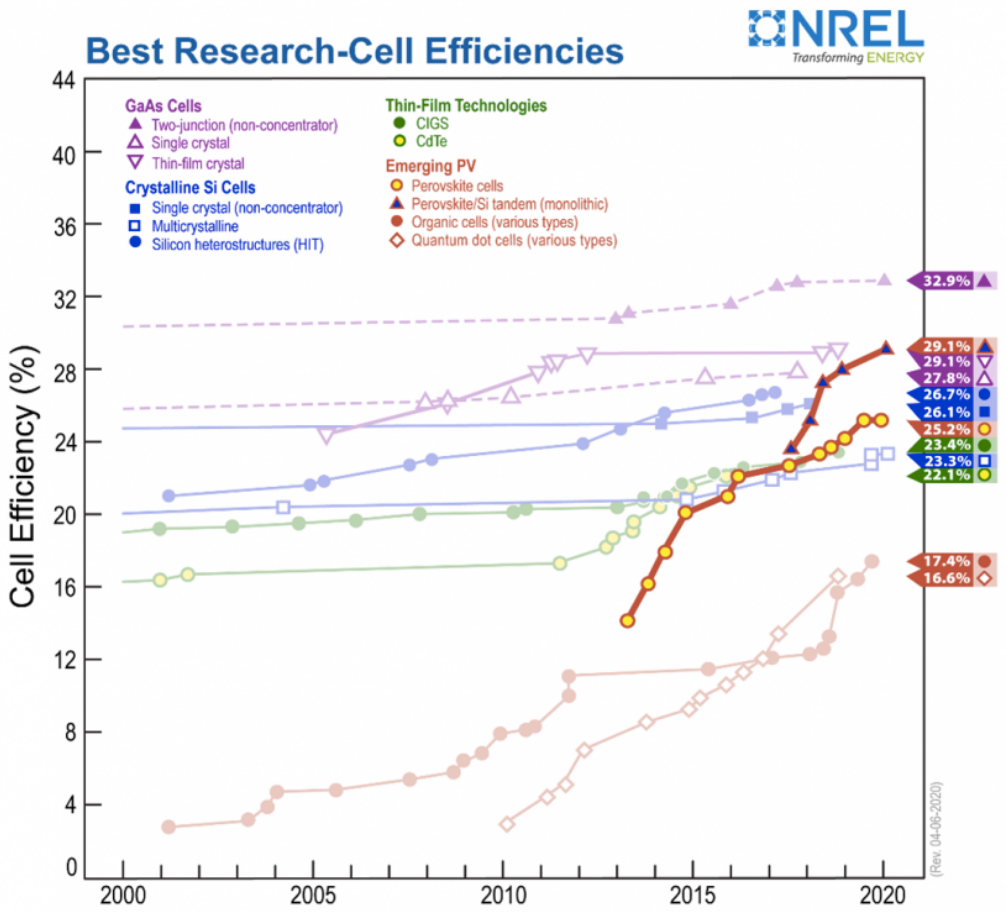


***Figure 1.*** *Cell efficiencies of existing solar technologies over the past 20 years (Office of Energy Efficiency and Renewable Energy, n.d.).*

### a. Silicon

The currently leading material used in the production of photovoltaic cells is crystalline-silicon. According to the National Renewable Energy Laboratory, photovoltaics comprised of either mono- or multi-crystalline silicon comprise 94% of those produced in 2014 (Woodhouse et al., 2016). Silicon's widespread use can be attributed to the material's high PCE, which was recorded at 31% in 2019 for thin-film solar cells (Bhattacharya & John, 2019). This efficiency exceeds that of any other current or emerging material used in solar cells, when considering cell designs comprised of a single absorber material. The downfalls of this material come from the production processes currently used, which are either costly or cause a loss of material due to slicing techniques. In two of the common processes for silicon crystallization, the Czochralski and Bridgman processes, approximately 50% of the initial material will be lost as dust when slicing the material into thin wafers (Ranjan et al., 2011). Though the Bridgman process is less

costly compared to the Czochralski process, this loss of material brings in notable additional costs to recycle lost material for either process. Before the material can be crystallized however, the silicon needs to go through a refining process multiple times. This is because the silicon used in solar cells demands a very high level of purity, at 99.999999999% (De Rooij, n.d.).

Though silicon itself is not toxic to the environment, there are toxic properties that come from the additional ingredients in crystalline-silicon panels. Some such materials used alongside silicon in these panels include polymers, silver, copper, boron, phosphorus, tin, tin oxide and lead (Kwak et al., 2020). Leaching tests performed based on the requirement of the Toxicity Characterization Leaching Process found that these panels produced results that approached and exceeded acceptable limits (Nover et al., 2017). This included the leaching of silver, tin, aluminum, copper and lead from amorphous silicon and crystalline silicon modules (Nover et al., 2017). There are also toxicity risks related to silica dust. An example of this is silicosis, which results from long-term exposure to even low amounts of silica dust. Symptoms can range from difficulty breathing to severe, fatal lung inflammation (*Silicosis*, n.d.).

### b. Thin-film Technologies: CdTe

Cadmium telluride is currently the second most common material used for solar cells. CdTe has a direct bandgap, making it ideal for the conversion of sunlight to energy, with a tunable bandgap around 1.45 eV (Britt & Ferekides, 1993). In 2016, First Solar recorded an efficiency for CdTe thin-film solar cells of 22.1% (Osborne, 2016). Cadmium is an abundant resource given that it is a byproduct of the mining industry, but telluride is much harder to acquire, which offsets any cost benefits of cadmium. Both cadmium and telluride are toxic compounds, with cadmium being recognized as a toxic substance by the US Environmental Protection Agency (EPA), meaning there are limits set for acceptable levels of cadmium in drinking water (Ramos-Ruiz et al., 2017). Tellurium, while not regulated by the EPA, can have significant effects and cause damage to vital organs such as the kidney, and exposure can occur through production fumes as well as through water and soil (Vij & Hardeij, 2012) from landfill leachates.

### c. Perovskite Materials

Thin-film cells that utilize direct-gap absorbers may be potentially cheaper than silicon solar panels, although efficiencies may not be as high (Dirjish, 2012). Perovskites are being

applied more frequently in the form of thin-film solar cells. Perovskites can convert light to energy with comparable efficiencies to today's best commercially available silicon-based solar panels. Thin films have the capability to be a groundbreaking new technology, because they only use a fraction of the material of traditional, silicon-based solar panels - a piece 100 times thinner (Peleg, 2018). As thin films demonstrate high plasticity, they should also be softer and more flexible than the rigid, fragile crystalline-silicon solar panels.

The focus is shifting to perovskite-based solar panels, which are cheaper and faster to make. The loose definition of a perovskite is a material with a crystal structure of the form $ABX_3$, shown in Figure 2, typically containing an organic cation, a metal, and a halide.

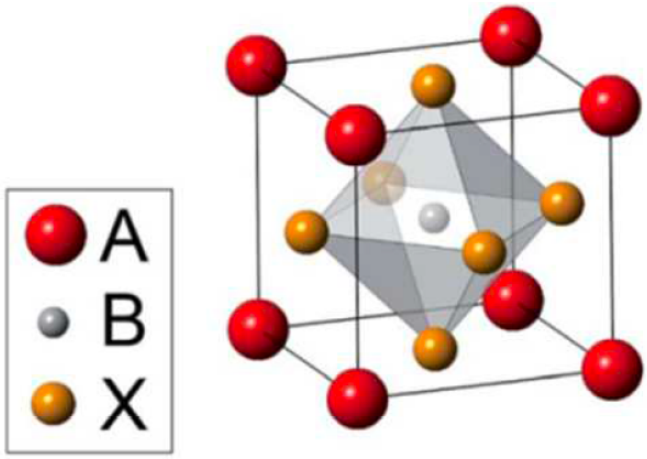


***Figure 2.*** *Crystal structure of an $ABX_3$ perovskite (Luo, 2014).*

The most frequently studied perovskite photovoltaics are lead-based organic-inorganic hybrids, with tin as a common substitute for lead. As of 2018, there has been a rapid increase in PCE of halide perovskite solar cells (PSCs) from 3.8% to 22.1% (Cao et al., 2018). There are numerous advantages to the use of PSCs. They have long carrier diffusion lengths, on the scale of μm, indicating that photogenerated carriers could be efficiently collected by external contacts (Saliba et al., 2016). Figure 3 depicts carrier generation, which involves the input of energy for electron excitation, as well as recombination, where the electron returns to its ground state.

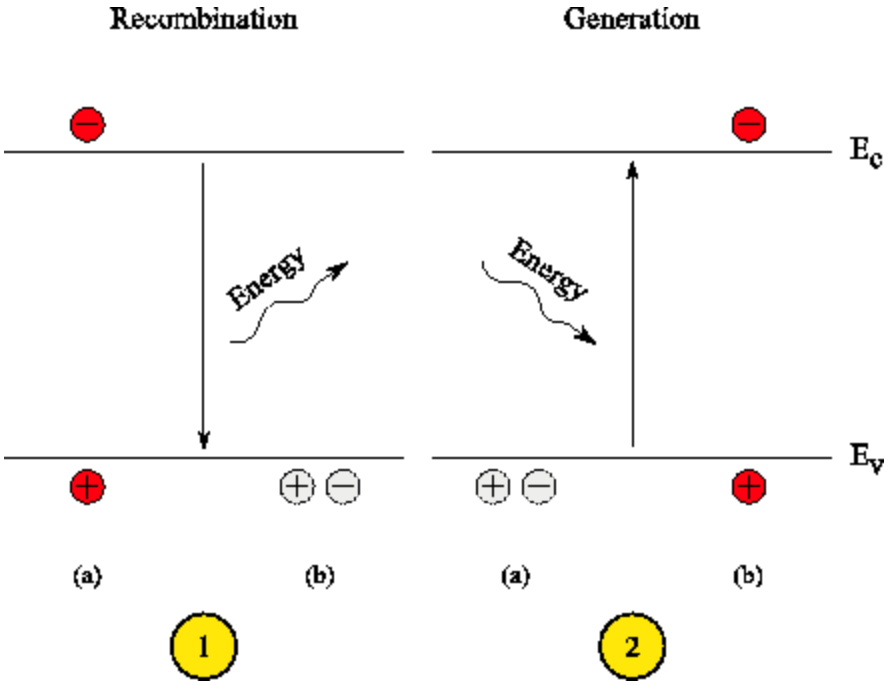


***Figure 3.*** *Depiction of carrier recombination and generation (Entner, n.d.).*

Perovskites also have tunable bandgaps in the range of 1.1-2.3 eV, which can be achieved through interchanging cations, metals, and/or halides, allowing for flexibility in design and optimization (Saliba et al., 2016). Their light absorption potential is promising, and they involve low-cost fabrication techniques while maintaining a relatively high efficiency (Shi & Jayatissa, 2018). They have the potential to be used as an independent solar cell material, as well as in tandem with a silicon solar cell to help maximize efficiency, shown in Figure 4 (Office of Energy Efficiency and Renewable Energy, n.d.).

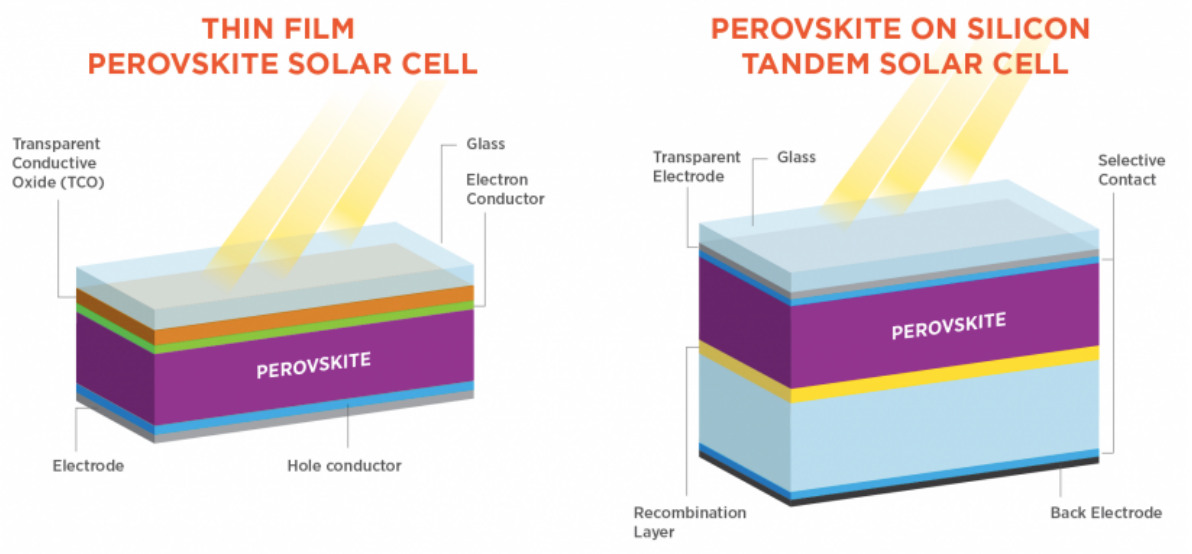


***Figure 4.*** *Thin film perovskite solar cell and perovskite on silicon tandem solar cell (Office of Energy Efficiency and Renewable Energy, n.d.).*

### *Problems with lead- or tin-based inorganic-organic hybrid*

Before wide-spread implementation and industrialization can occur, there are a few drawbacks that need to be addressed with perovskite-based photovoltaics. Lead-based perovskites have toxicity concerns throughout the production chain, and many perovskites are relatively unstable (Shi & Jayatissa, 2018). Upon moderate exposure to external stimuli like humidity, oxygen, elevated temperature, or a combination thereof, the photovoltaics (PVs) are likely to degrade into harmful compounds carrying heavy metals which may readily leach into the environment as the result of the structural failure of a photovoltaic module (Babayigit et al., 2016). There are also human-health concerns when manufacturing these PVs, the main sources of intoxication hazard are the starting compounds and solvents. Specifically, organic lead and tin compounds like the ones most frequently studied have a more significant health impact, as they can readily pass biological barriers to reach vital areas due to relatively high fat solubility (Babayigit et al., 2016). Not only are lead- and tin-poisoning concerns during the manufacturing of the solar panels, but this poses a risk for consumers both during use and at end-of-life. Structural integrity can be affected when the perovskite modules are placed in uncontrolled conditions, like a rooftop, leading to perovskite degradation and leakage of toxic chemicals into the immediate surroundings. This could involve reversion to starting products, which can then decompose further into compounds such as $PbI_2$, $PbBr_2$, $SnI_2$ or $SnI_4$(Babayigit et al., 2016). There

is then concern for local toxicant accumulation, leading to acidification of environments and degradation of ecosystems. At the end of life of the solar cells, there are concerns about the recycling of lead-based products, which although possible, poses similar health concerns to those that arise during the fabrication process (Babayigit et al., 2016). The challenges that still exist and must be addressed for widespread implementation of any perovskite material are listed in Figure 5. The top priorities are PCE and stability and degradation, but manufacturing and bankability are also important (Office of Energy Efficiency and Renewable Energy, n.d.).

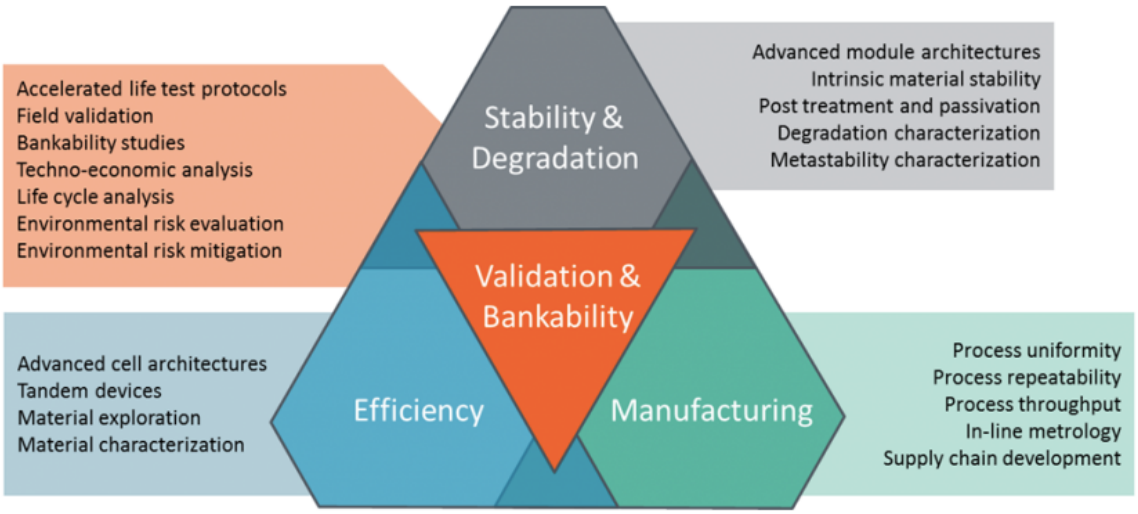


***Figure 5.*** *The challenges and future research routes of perovskite solar cell industrialization (Office of Energy Efficiency and Renewable Energy, n.d.).*

### *$Cs_2TiBr_6$*

Solar cells fabricated with lead-free perovskites and perovskite-like materials exhibit limited efficiency, and development of stable, appropriate compounds is not a straightforward task (Euvrard et al., 2020). For example, Sn- and Ge-based perovskites are unstable due to propensity to oxidize in air, and Bi and Sb-based perovskites show good stability but poor PCEs (Euvrard et al., 2020). To counteract the toxicity concerns of lead-based perovskites and the shortcomings of other alternatives, we have been looking into the efficiency potential of a Ti-based, completely inorganic perovskite-like material that eliminates both the volatile organic ions and introduces a less toxic metal base. This new material, $Cs_2TiBr_6$, has favorable band gaps of ~1.8 eV or 689 nm, in the red portion of the visible spectrum, resulting in high optical absorption of a large portion of the sunlight that reaches the Earth's surface (Ju et al., 2018). It

also has been shown to have carrier-diffusion lengths exceeding 100 nm, necessary for extracting free carriers following light absorption (Chen et al., 2018; Euvrard et al., 2020). Titanium, the metal used as a replacement for lead and tin, is earth-abundant, biocompatible, and considered nontoxic. $Cs_2TiBr_6$-based PVs with efficiency as high as 3.3% have been reported (Chen et al., 2018, Ju et al 2018). It is also completely inorganic, and the titanium cation exists in the preferred and stable +4 oxidation state.

$Cs_2TiBr_6$ is often referred to as a perovskite-like or a double perovskite, as its crystal structure does differ slightly. Figure 6 below shows the structure of a perovskite, with general form $ABO_3$, as well as the structure of a double perovskite.

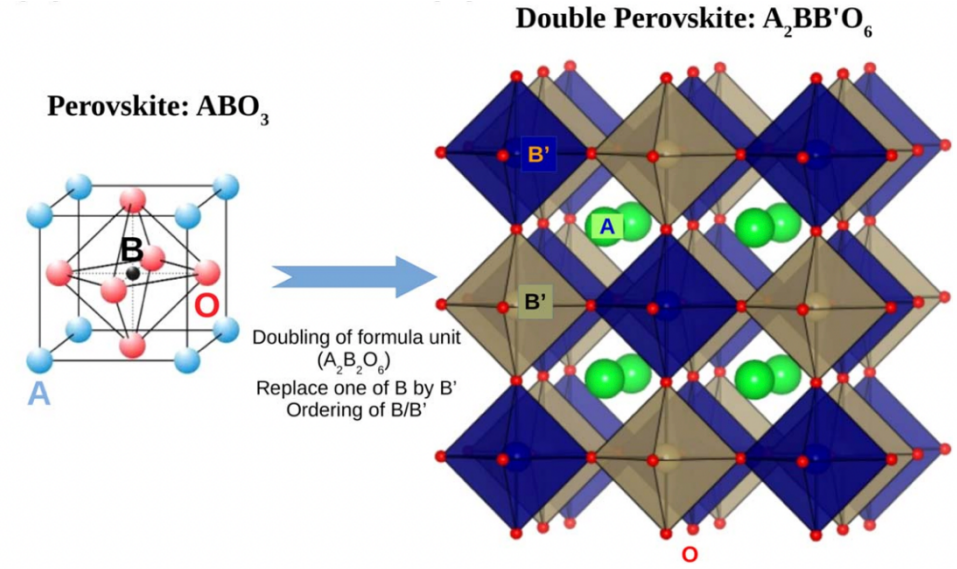


***Figure 6.*** *The general structure of a perovskite (left) and a double perovskite (right) (Saha-Dasgupta, 2020).*

In a closely related structure to perovskites and double perovskites, $Cs_2TiBr_6$ has a structure that is better defined as an antifluorite. The unit cell of the canonical antifluorite, $Na_2O$, has four stoichiometric $O^{2-}$ anions occupying its unit cell corners, faces, and middle while eight $Na^+$ cations occupy all the accompanying tetrahedral holes. Several antifluorite compounds exist in which the anion is polyatomic, such as potassium hexachloroplatinate where each anion position is held by $(PtCl_6)^{2-}$ octahedra while $K^+$ cations reside in the tetrahedral holes. The structure of $Cs_2TiBr_6$ demonstrates strong similarities to $K_2PtCl_6$ and is shown below in Figure 7 where the green elements represent cesium, the blue elements represent titanium, and the brown elements represent bromine.

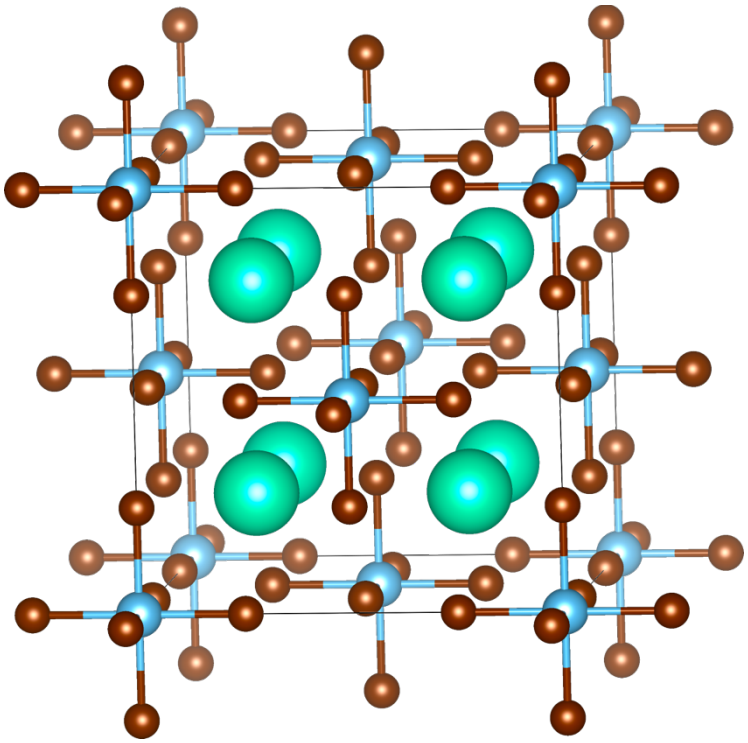

*Figure 7. The structure of $Cs_2TiBr_6$, where the green elements are cesium, blue are titanium, and brown are bromine.*

At first glance, the compound antifluorite structure resembles a double perovskite, but subtle differences exist. For $Cs_2TiBr_6$, the locations of the bromine and the cesium mirror the format of a double perovskite, but $Cs_2TiBr_6$ lacks the second metallic component, represented by B' in the depiction of the double perovskite. This is because titanium carries a +4 charge rather than the expected +2 charge of the metallic component of a perovskite. For the purposes of this report, we will simply refer to $Cs_2TiBr_6$ as a perovskite-like material.

To date, reports of $Cs_2TiBr_6$'s stability under ambient conditions have been contradictory. Many lead-free perovskites and perovskite-like materials are unstable when exposed to heat, oxygen, moisture, and other environmental factors (Schileo & Grancini, 2021; Correa-Baena et al., 2017). According to some reports, the decomposition of $Cs_2TiBr_6$ starts at temperatures as high as 400 °C, limiting its susceptibility to ambient degradation and conversion to titanium dioxide (Chen et al., 2018). In another study, solution synthesized $Cs_2TiBr_6$ powder was found to be strongly hygroscopic and highly unstable in air (Euvrard et al., 2020). Mendes et al. (2020) also found that large-grain $Cs_2TiBr_6$ crystals are unstable toward oxidation and formation of interfacial CsBr in air ambient. Mendes et al. (2020) further established some

electronic properties and band-edge energies of nascent, oxide-dominated $Cs_2TiBr_6$ and pure $Cs_2TiBr_6$ cleaved in ultra-high vacuum environments differ significantly.

In this study, our focus was on intrinsic properties of $Cs_2TiBr_6$ in both single crystalline and thin film form. All samples were therefore sealed in a quartz cell under dry $N_2$ atmosphere to minimize oxidation.

### *Electronic structure of $Cs_2TiBr_6$ from UV-visible spectroscopy*

The band gap of a material corresponds to the material's threshold for optical absorption and the energy of optical emission. The type of band gap of a material, direct or indirect, determines radiative lifetime and therefore luminescent efficiency (Fox, 2001). Materials with direct band gaps emit photons when an electron at the bottom of the conduction band recombines with a hole at the top of the valence band. In a direct band gap material, the minimum point of the conduction band and the maximum point of the valence band sit at the same point in the Brillouin zone, as seen in Figure 8, and only a photon needs to be emitted for conservation of energy (Fox, 2001). Direct band gap materials have a short radiative lifetime and therefore a high luminescent efficiency. These materials lend themselves to both light absorption as well as light emission. Materials with indirect band gaps on the other hand, are typically bad for light emission, and are rarely used for emission unless there is no alternative. These materials have conduction and valence bands that are at different points in the Brillouin zone (Fox, 2001), as seen in Figure 8. This means that when an electron from the conduction band is injected into a hole in the valence band, a phonon must be emitted with the photon to conserve momentum. This makes this process with indirect transmissions a second-order process with a radiative lifetime that is longer than those of direct transmission, and therefore a smaller luminescent efficiency (Fox, 2001).

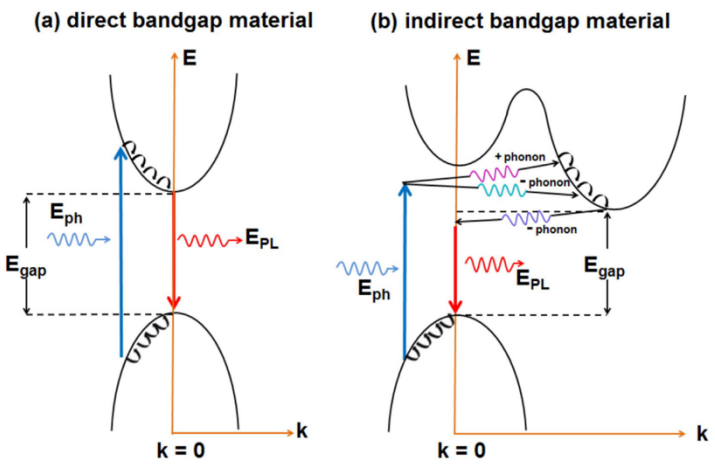


***Figure 8.*** *Interband transitions in (a) direct bandgap and (b) indirect bandgap materials (De los Reyes, 2015).*

Energy structure of a material can also be modified by interactions between the charge carriers. An example of such interaction is the formation of excitons, which are correlated electrons and holes that remain bound to each other (Potter & Simmons, 2021). When a photon with energy above the semiconductor's bandgap energy is absorbed by a bound electron in the valence band, it becomes free and moves into the conduction band, leaving behind a free hole. The electrostatic force between the electron and the hole results in a formation of a bound state, similar to a hydrogen atom (Williams, 2019). There are two types of excitons: Wannier-Mott excitons, or free excitons, and Frenkel excitons, or bound excitons. Figure 9 illustrates the difference between free excitons and tightly bound excitons (Fox, 2001). Wannier-Mott excitons are frequently observed in semiconductors. Their stability is determined by binding energy, and optical features such as strong absorption or efficient emission by the excitons is often observed. While the exciton binding energy in $Cs_2TiBr_6$ has not yet been reported, we note here that other inorganic perovskites $CsPbCl_3$ and $CsPbBr_3$ have exciton binding energies on the order of 50-100 meV, making them stable at room temperature and resulting in optical emission by excitons bound to a higher-lying defect state within the conduction band (Sebastian et al., 2015).

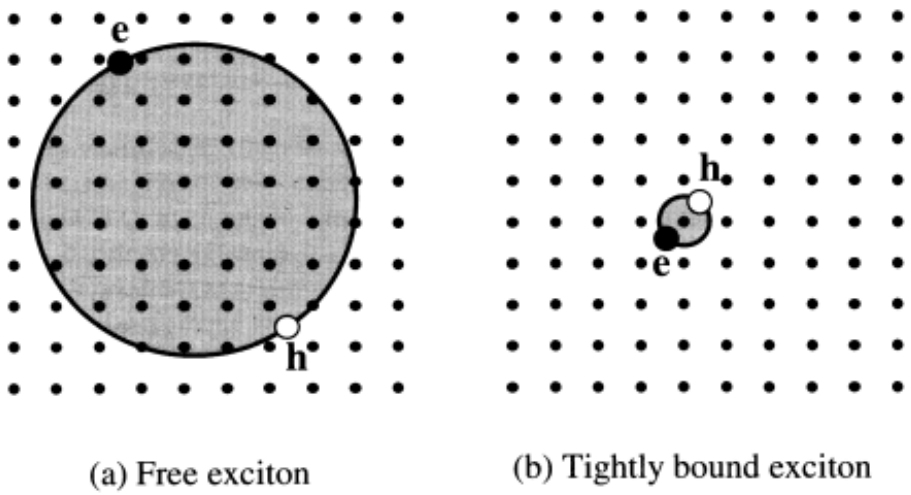


***Figure 9.*** *Depiction of a free exciton (a) and a tightly bound exciton (b) (Fox 2001).*

One way to experimentally obtain the band gap of a material and determine its optical properties is by using ultraviolet-visible spectroscopy (UV-Vis). UV-Vis is an analytical technique that measures the amount of light that is absorbed by or transmitted through a sample. This can indicate the sample's composition (Tom, 2021). Of relevance to our project is the ability to calculate band gaps through use of UV-Vis spectra and the Tauc plot (Makuła et al., 2018). Figure 10 illustrates an example of a Tauc plot showing the determination of thin film $Cs_2TiBr_6$'s direct band gap.

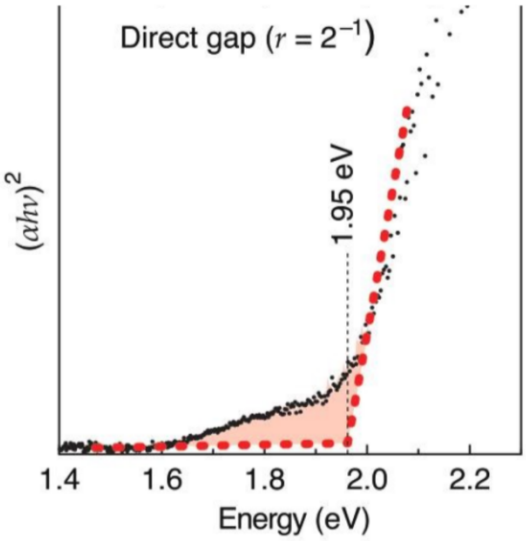


***Figure 10.*** *UV-Vis-derived Tauc plot for a thin film sample (Mendes et al., 2020).*

The absorption coefficient multiplied by photon energy to the power of 1/r is represented on the y-axis of the Tauc plot, where r= 2 to determine indirect band gaps and r = 1/2 to determine direct band gaps. From here, the onset can be extrapolated and fit to a line. The solid red portion on the figure above is the Urbach tail, which represents absorption due to defect states.

## 2. Photoluminescence Spectroscopy

Photoluminescence spectroscopy (PL) quantifies the recombination of free carriers in a semiconductor, which can elucidate its electronic structure. It is contactless and nondestructive, using photons to probe a material and causing the photoexcitation and release of photons from that material (Ye & Barron, n.d.). This process and the necessary components for such an experiment are shown in Figure 11. PL applications include band gap determination, impurity levels and defect detection, recombination mechanisms, as well as material quality/structure/crystallinity (HORIBA, n.d.). Band gap determination is one application of PL that is particularly useful to this project. The band gap of a material determines the photovoltaic (PV) efficiency of a material. Materials with very high bad gaps are unable to absorb most of the solar energy reaching the Earth' surface and thus are not useful for PV applications. At the same time, materials with very low band gaps convert an excess of energy between the band gap and photon energy into heat, resulting in much of the solar energy wasted (Penn State Department of Energy and Mineral Engineering, n.d.). The optimal band gap energy for PCE is between 1.80-1.88 eV (Jarosz et al., 2020).

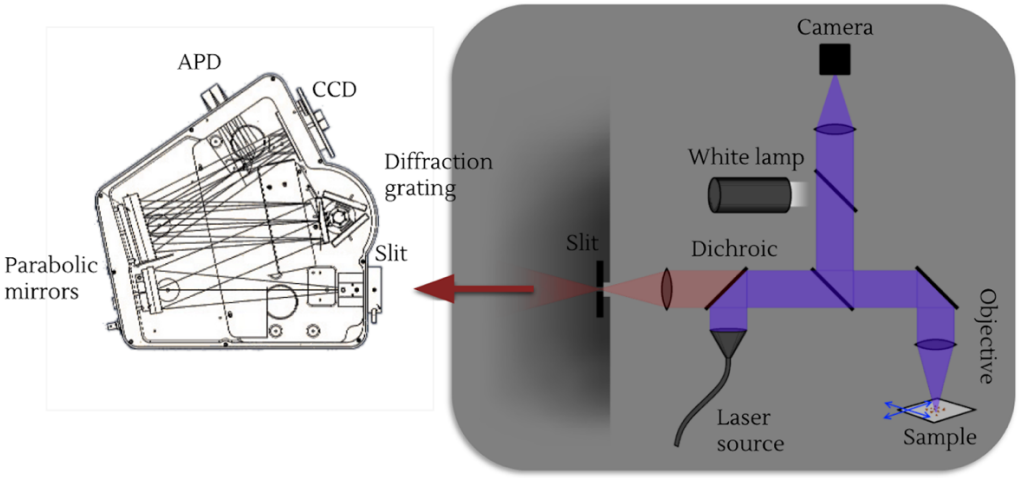


***Figure 11.*** *Photoluminescence spectroscopy optical setup (Fitzgerald, n.d.).*

PL spectra can also help in determining the material's quality by identifying defects and impurities in that material that could affect device performance. Defect levels are associated with different photoluminescence energies that can be observed to identify and quantify defects (Ye & Barron, n.d.). All semiconductors contain defects, either on purpose or by accident, in the form of impurities, native defects, and extended defects, which affect a broad range of applications (McCluskey & Janotti, 2020). There are two types of defects - native defects, which involve only the atoms of the host crystal, and extrinsic defects, which involve impurity atoms (McCluskey & Janotti, 2020). When an impurity is deliberately introduced into a semiconductor, it is referred to as a dopant (McCluskey & Janotti, 2020). A specific type of defect is a grain boundary, which is the interface between two grains in a polycrystalline material (*Grain Boundary (GB)*, 2020). They tend to decrease the electrical and thermal conductivity of the material and are preferred sites for the onset of corrosion (*Grain Boundary (GB)*, 2020).

After the photon excites an electron from the valence to the conduction band, different processes can take place, with their likelihood determined by the type of the material (e.g., direct vs indirect band gap), presence of defects that can trap carriers, probability of exciton formation and others. Over time, an excited electron returns to its ground state in the valence band in a process called recombination. If this process is accompanied by the emission of a photon, this is known as radiative recombination. If instead excess energy dissipates in the form of emitted phonons (or heat), recombination is non-radiative. Radiative recombination involves the release of a photon when an electron combines directly with a hole in the valence band, is dominant in

direct bandgap semiconductors, whereas $Cs_2TiBr_6$ and silicon, the current leading material in solar panels, exhibit indirect bandgap properties (*Types of recombination*, n.d.). In indirect gap semiconductors, the transition between the electron at the bottom of the conduction band and the hole at the top of the valence band does not conserve momentum and thus requires a third particle, typically a phonon, or a quantum of crystal lattice vibration, to carry away momentum. This process involves three particles and is therefore not probable, resulting in low PL efficiencies in indirect gap semiconductors. Another type of recombination is defect recombination, which is a two-step process involving an electron trapped by an energy state in the forbidden region introduced through defects. If a hole moves up to the same energy state before the electric is thermally re-emitted into the conduction band, then they recombine (*Types of recombination*, n.d.). A third type of recombination is Auger recombination, which involves three carriers. Here, an electron and a hole combine, and the energy is given to an electron in the conduction band, which then thermalizes back down to the conduction band edge (*Types of recombination*, n.d.). This type of recombination is most important at high carrier concentrations, caused by heavy doping or high-level injection under concentrated sunlight. In the case of silicon-based solar cells, Auger recombination limits the lifetime and efficiency of the cell - the more heavily doped the material is, the shorter the Auger recombination lifetime (*Types of recombination*, n.d.).

Time-resolved PL spectroscopy is used to monitor light emission from a sample as a function of time after excitation (De los Reyes, 2015). Using a short, pulsed laser excitation, it is possible to determine the decay kinetics of light emitting materials by recording the emission intensity over different delay times after excitation (De los Reyes, 2015). In this work, we used time-correlated single photon counting (TCSPC) to record PL decays, as described below in the methodology.

In carrying out TCSPC measurements, it is important to consider excitation repetition rate. High repetition rates of the pulsed source increase the count rates and improve the signal to noise ratio. However, the time between each excitation must still be longer than the relaxation time of the carrier to the ground state (De los Reyes, 2015). Furthermore, PL count rate needs to be less than 5% of the laser repletion rate so that probability of two photons emitted by the sample following a single laser pulse is low. This avoids so-called ‘pulse pile-up’, an artefact that results in the radiative recombination rate appearing higher than it is. In our measurements, we could

change the repetition rate of the laser from 1 kHz to 20 MHz. Determining the decay kinetics of light emitting materials using PL is important given that these properties in a solar cell material can affect its quality and how the device performs.

## 3. Integrating Perovskites into Solar Devices

Solution processing is a common method being used to create perovskite thin-film solar cells. Perovskite solar cells have a stack-like structure, with layers of perovskite thin-films in between an electron transporting layer and a hole transporting layer (Saki et al., 2021). Solution processing is a common method used for creating thin-film devices, and it works by depositing a material from a solution onto the device surface repetitively, creating layers. This process is a highly scalable one and allows for the potential of very low-cost manufacturing (Marsh, 2020).

The thin perovskite films are prepared through a low-temperature vapor-based method (Chen et al., 2018). A method being looked at by the Duke group is Resonant Infrared Matrix-Assisted Pulsed Laser Evaporation (RIR-MAPLE). This technique was adapted from MAPLE and involves freezing a solution containing the molecular building blocks for the perovskite, and then blasting the frozen block with a laser in a vacuum chamber (Peleg, 2018). The vaporized portion of the frozen target travels upward and coats the bottom surface of an object overhead, which could include a component in a solar cell. After enough of the material has built up, the product is heated to crystallize the molecules and set the thin film in place (Peleg, 2018).

By restructuring the way that perovskite solar cells are designed, efficiency can be massively improved for increased deployment opportunities. As previously discussed, the cells are made of layers of materials that are sandwiched together, with the top and bottom layers key to the conversion of sunlight to electricity (National Renewable Energy Laboratory, 2021). Suggested new architecture involves increasing the area exposed to the sun by putting these two layers side-by-side on the back of the cell. This, theoretically, would lead to higher efficiency due to greater sunlight absorption. This design is called complementary interface formation (National Renewable Energy Laboratory, 2021). This removal of layers also enables seamless integration of solar panels into buildings, approving the aesthetics of the cell and “camouflaging” the solar cell. This has many positive implications for widespread implementation (National Renewable Energy Laboratory, 2021).

## 4. Sustainability

The definition of sustainability is multi-faceted. There are a variety of existing definitions, but to ensure a society and planet that is suitable for future generations, they all involve the same three pillars: economy, equity, and environment (UCLA, n.d.; McGill University, n.d.). In 1987, the United Nations defined sustainability as "meeting the needs of the present without compromising the ability of future generations to meet their own needs" (United Nations, n.d.). Similarly, the EPA committed the United States to sustainability in 1969, declaring that we would "create and maintain conditions under which humans and nature can exist in productive harmony, that permit fulfilling the social, economic and other requirements of present and future generations" (US EPA, 2014). Often, with green development, many have claimed that the current economic system must be reformed to allow for radical climate mitigation (Söderholm, 2020). The Green Economy is a vision that can generate economic development and improvements in people's lives in ways that will also allow for environmental and social well-being (Söderholm, 2020). This involves adopting and promoting sustainable technologies. When considering new technologies that may be more environmentally friendly, we also need to consider how equitable and economically viable their impacts are.

### a. Problems with conventional solar panels

Solar power is a frequently discussed alternative to fossil fuel energy and is increasingly important considering the recent urgency to switch to non-polluting sources. There are a variety of ambitious goals for time frames for full transitions to renewable energy, but according to the US EIA, in 2020, renewable energy sources accounted for only about 12% of total U.S. energy consumption (US EIA, 2021). Green energy sounds like an ideal substitute, but as with all material and technological substitution, it comes at a cost to both the environment and public health. These sources of renewable energy involve resources such as copper, lithium, cobalt, and other harmful heavy metals with sources primarily in developing countries. This only serves to widen the gap between the West and the developing world. Although it is the most abundant, free, and sustainable energy source, the cost of harvesting solar power using conventional photovoltaics (PVs) remains high compared to fossil-fuel energy sources (Ju et al., 2018).

Solar power has several negative environmental impacts that are often not considered when discussing alternative energy technologies. In general, there are a variety of life-cycle carbon dioxide emissions to consider, such as those released during manufacturing, materials transportation, installation, maintenance, and decommissioning. Solar facilities raise concerns about land degradation and habitat loss. Opportunities to share land with agricultural uses are also diminished, whereas alternatives such as wind facilities maintain the option of agricultural land usage. (Union of Concerned Scientists, 2013). For wide-scale deployment, one possible way around this issue is to place solar facilities on lower-quality land, or to employ them on smaller scale locations like homes or commercial buildings (Union of Concerned Scientists, 2013). Water use during the manufacture of solar PV components is also intensive - it is used for cooling components and in wet-recirculating technology (Union of Concerned Scientists, 2013).

A significant problem with the production of solar panels of all varieties is the handling of hazardous materials. For example, even in the production of silicon solar panels, hazardous materials are used to clean and purify the semiconductor surface, such as hydrochloric acid, sulfuric acid, and hydrogen fluoride (Union of Concerned Scientists, 2013). The amount and type of chemical used depends on the type of cell, size of the silicon, and the amount of necessary cleaning. Thin-film PV cells, such as gallium arsenide, copper-indium-gallium-diselenide, and cadmium-telluride, include the use of even more toxic materials than traditional silicon PVs (Union of Concerned Scientists, 2013). Similarly, perovskite solar panels commonly contain toxic heavy metals, such as lead and tin. Due to these problems, widespread commercialization of solar panel technologies requires regulations on manufacturers to ensure that workers aren't harmed by exposure (Union of Concerned Scientists, 2013).

In addition to the plethora of environmental issues raised through the implementation of solar panels, there are also potential negative social implications. Besides the concerns for worker safety when handling toxic materials, there is also potential for noise and visual intrusions, water and soil pollution, labor accidents, and socio-economic effects regarding the equitable distribution of these technologies and concerns about sourcing materials (Tsoutsos et al., 2005).

### *a.1 Leading Materials*

As discussed previously, there are a variety of different solar panel materials currently on the market, all with varying efficiencies. These relative efficiencies were given previously in Section I, Figure 1. Some commonly used materials for solar panels include crystalline and amorphous silicon, gallium arsenide, and various organometallics like soluble platinum. Crystalline silicon exhibits the highest efficiency and makes up about 90% of solar cell semiconductors in 2018 (Danylenko, 2018). Amorphous silicon is far less efficient and degrades when exposed to sun rays. Gallium arsenide has the potential to be highly effective with a better band gap than silicon, but gallium is extremely rare, and arsenic is toxic, making the extraction and life cycle of the materials problematic (Danylenko, 2018).

The leading material, crystalline silicon, not only has a high PCE but is also easy to source (Woodhouse et al., 2016). Silicon is the second most earth-abundant element, found abundantly in certain rocks, sand, and soil (De Rooij, n.d.). When used in the electronics industry, the silicon is highly purified and produced by reduction processes. This involves rigorous refinement and purification, involving zone refining, distill refining, and electrolytic refining (De Rooij, n.d.). This makes the process expensive and energy intensive, thus imposing costs on both the environment and the economy. Silicon-based solar cells also contain various additional ingredients that have the potential to leach into the environment under different pH conditions. These ingredients include glass, polymers, silver, copper, boron, phosphorous tin, tin oxide, and lead (Kwak et al., 2020). The heavy metals leached from these cells can end up in the environment and have proven to exhibit partial ecotoxicity. They could potentially affect water and soil sources, and thus prove harmful to human health while also disrupting surrounding ecosystems (Kwak et al., 2020). With a limited number of studies conducted on toxicity of silicon-based solar panels, additional negative impacts may also exist.

Alternative materials have emerged due to their low costs and simple manufacturing techniques, such as perovskite-based solar cells. Various inorganic-organic halide perovskites have been developed and applied to PV devices, many containing heavy metals such as lead and tin (Kwak et al., 2020).

### *a.2 Perovskite Alternatives*

Recent technologies have brought perovskite solar cells to an efficiency level that rivals silicon PVs on a laboratory scale. These perovskites are most often organometal halide perovskites (OHPS), with the perovskite structure $ABX_3$ where A is most commonly an organic compound of $Cs^+$, B is Pb or Sn, and X is I or Br (Babayigit et al., 2016).

As discussed in the previous chapter, perovskites have favorable intrinsic properties such as ambipolarity, high charge-carrier mobilities, high diffusion lengths, and high absorption coefficients (Babayigit et al., 2016). Hybrid halide perovskites are the new generation of photovoltaics, due to their comparable efficiencies, ease of fabrication, flexibility, and versatility (Schileo & Grancini, 2021). They also have an energy payback time (EPBT), which is the time it takes to generate the amount of energy used to produce the PV, of just a few months, whereas silicon solar panels have an EPBT between 1.5-4.4 years (Schileo & Grancini, 2021).

Perovskite solar cells (PSCs) also have the potential for rapid small-area device advancement and expansion of PV technologies to increase efficiency beyond that of single-junction devices (Rong et al., 2018). PSCs have shown to work well as top cells of tandem solar cells in conjunction with existing PV technologies. Additionally, they have exhibited industry standard lifetimes that are greater than 10,000 hours, or an equivalency of 10 years of outdoor use in most locations (Rong et al., 2018).

Currently, the challenges faced by perovskite solar cells include stability, upscaling, and reliability (Rong et al., 2018). With efficiencies already greater than 20%, long term stability is one of the key issues impeding rapid commercialization (Correa-Baena et al., 2017). There are also concerns about the potential of long-term hazards posed to the environment. For example, during the end of life of the solar cells, dismantling a PSC could potentially be more demanding (Espinosa et al., 2015). Furthermore, there are questions about how cost-effective PSCs would be in a broader scaling scenario (Espinosa et al., 2015).

#### **a.2.1** Lead-based hybrids

Despite PSCs being low cost and simple to fabricate, the most widely used perovskites contain lead. Concerns over lead toxicity put a strain on public perception and acceptance (Babayigit et al., 2016). The leaching of lead and other components, such as iodine, into the

environment could be detrimental to ecosystems and public health (Kwak et al., 2020). This degradation can occur upon moderate exposure to external stimuli like humidity, oxygen, and elevated temperature, or through the general structural failure of a PV module (Babayigit et al., 2016). The most common alternatives to lead-based perovskites are tin-based perovskites; however, tin is also a heavy metal that can induce similar detrimental environmental and health effects. Even in the small quantities in which they're used in PSCs, potential exposure associated with large-scale implementation should be treated with caution (Babayigit et al., 2016).

Lead and tin toxicity can have severe effects on the human body, with three possible routes of intake: gastrointestinal, respiratory, and dermal (Babayigit et al., 2016). These routes, as well as the way the heavy metals are then distributed within the human body, are detailed in Figure 12. It also indicates how they are excreted from the human body. An excretion containing traces of these metals is breast milk, which could be damaging to the health of infants who are more susceptible to the effects of heavy metal intoxication in the early stages of development (Babayigit et al., 2016).

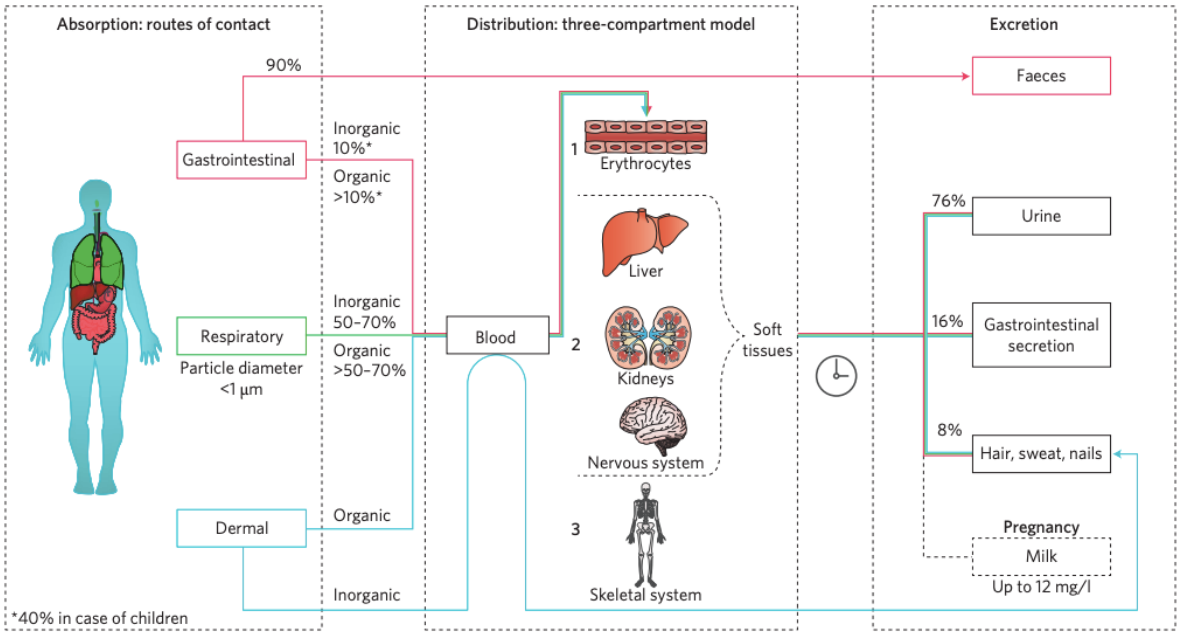


***Figure 12.*** *The routes of intake of lead in the human body and their subsequent distribution and excretion (Babayigit et al., 2016).*

Lead ions cause damage through mimicry of essential elements such as calcium, zinc, and iron. In soft tissues, this results in impaired functionality of enzymes and receptors,

interferes with haem activities that are essential for aerobic processes in blood, and fixation to bones after prolonged exposure (Babayigit et al., 2016). The ability of compounds to pass into the bloodstream from the respiratory system is heightened when the compound is organic due to its solubility in fat (Babayigit et al., 2016). Organic compounds are also more volatile, thus affecting the efficiency and stability of these PSCs. Figure 13 shows the structure of the perovskite, including the volatile organic compounds and the toxic heavy metals. For lead, there was originally a threshold of a maximum of 5ug/dl in blood, which involves an intake of 2.5 mg through ingestion or 0.5 mg through inhalation. This has since been revoked, since even lower values can lead to effects in children and neurological deficiencies in adults through chronic exposure and acute uptake (Babayigit et al., 2016).

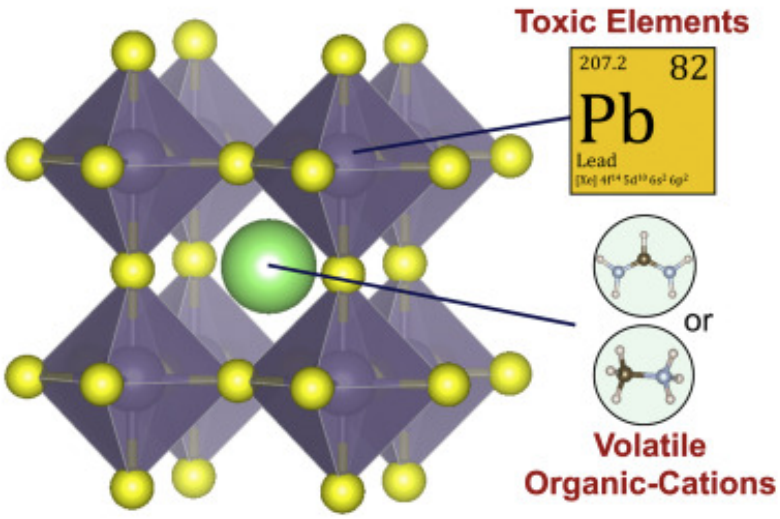


***Figure 13.*** *The structure of a typical lead-based organic-inorganic hybrid perovskite (Babayigit et al., 2016).*

The toxicity of tin is more complex and less well-studied than lead-poisoning. Due to the low redox potential of tin, rapid oxidation occurs in ambient atmospheres (Babayigit et al., 2016). Inhalation and ingestion are common routes of intake, where inorganic tin compounds are more likely to pass into the bloodstream when small in diameter and water soluble. Up to 70% of inhaled inorganic tin compounds that are small enough to be inhaled at the level of the alveoli can be transported to the blood (Babayigit et al., 2016). Similar to lead, Sn(II) and Sn(IV) interfere on a molecular level through mimicry of other elements, such copper (Babayigit et al., 2016). Because tin poisoning is less documented, there is no set threshold yet.

During the life cycle of a perovskite, there are five main stages that should be considered to determine the effects of specific toxic materials. These include raw material extraction, synthesis of starting products, fabrication, use, and decommissioning. The outcome may differ depending on the emphasis placed on each stage of the life cycle, as well as the chosen impact indicator (Babayigit et al., 2016). In one study conducted on the toxicity of lead in perovskites, the assumption was that all starting products and corresponding material extraction and synthesis have already been optimized in terms of health and safety. This was based on the chemicals' prior utilization on an industrial scale for other applications (Babayigit et al., 2016). Figure 14 shows the conclusions drawn about how lead may be harmful to health and safety during the remaining three steps of the life cycle, as well as how to mitigate the problem. Although detailed assessments of this technology are still developing, it is certain that the release of toxic species derived from perovskites will occur during all the above steps (Ju et al., 2018).

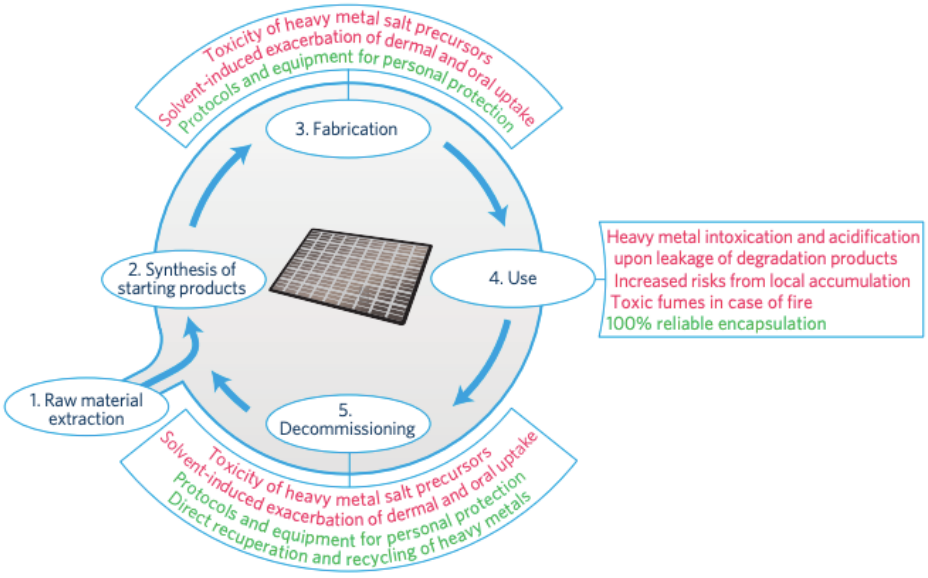


***Figure 14.*** *The possible effects of lead during the fabrication, use, and decommissioning steps of the life cycle of a solar panel using a lead-based perovskite component (Ju et al., 2018).*

Throughout the fabrication of the PV, the main intoxication hazards are the starting compounds and solvent. The potency is dependent on the chemical nature, which affects bioavailability and rate of uptake. During this phase, it's very difficult to fully enclose the lead vapor and dust that is released from processing facilities (Espinosa et al., 2015). To avoid these

hazards, sufficient protection is critical, such as necessary personal protective equipment (PPE) like gloves, masks, glasses, and waste storage. Generally, perovskite labs are not sufficiently employing use of this PPE (Babayigit et al., 2016). To avoid these health risks, there is also the potential for the creation of an environmental burden due to the use and disposal of PPE. Although assessing these effects is beyond the scope of this project, it is crucial to understand the repercussions of improving protective measures to accommodate the use of heavy metals in production.

During use, the structural integrity of the PV can be affected when the perovskite modules are placed in uncontrolled conditions, like a rooftop. This can lead to perovskite degradation and leakage of toxic chemicals into the immediate surroundings, reverting to the starting products and potentially decomposing farther (Babayigit et al., 2016). There is also the potential for module failure in the form of fire, which can lead to the emission of toxic fumes. Although recent estimations have shown that spilled lead from defective cells would be orders of magnitude smaller than that from emissions by other energy-related activities, researchers must still be exceedingly careful due to the danger of local toxicant accumulation. This process could have detrimental effects on public health and local ecosystems, such as acidification (Babayigit et al., 2016). For large scale implementation, there must be 100% reliable containment of degradation products from modules that lose structural integrity during useful life - this encapsulation must be resistant to extreme conditions.

Decommissioning is the final step of the life cycle to be considered. Lead is one of the most effectively recycled materials in the world. 80% of modern Pb usage goes into production of batteries, which have well-established recycling procedures, and the waste Pb from batteries can be recycled to produce $PbI_2$ for use in PSCs (Babayigit et al., 2016). Related risks to human health are like those of the fabrication stage; workers exposed to the products during the recycling process must be equipped with the required PPE to ensure their safety.

The effects of lead-based perovskites are not only limited to the impacts of lead toxicity on human health - there are also additional environmental and public health concerns that go beyond the issue of toxicity. Future work must go into complete life-cycle assessments of the environmental impact of lead-based perovskites. The release of lead substances during all phases of the PSCs life cycle will have a negative impact on the environment via land and water pollution, which could also lead to contaminants in the food chain (Espinosa et al., 2015). There

is also the potential for events that are environmentally catastrophic, such as fire or flooding, during the manufacturing, transportation, storage, and usage of lead-based PSCs (Espinosa et al., 2015).

### **a.2.2** Lead-free Halide Perovskites and $Cs_2TiBr_6$

Hybrid lead-based perovskites, as discussed, create concerns for both the wellbeing of the environment and human health. Lead-free perovskites offer a potential avenue to circumvent the lead toxicity problem. Tin-based perovskites, along with their additional toxicity concerns, exhibited much poorer performance and stability when exposed to oxygen and moisture (Espinosa et al., 2015). Potential lead-substituents must also be considered in terms of material abundance, toxicity, and environmental impact (Schileo & Grancini, 2021). A lot of lead-free perovskites display instability towards heat, oxygen, moisture, and other environmental factors (Schileo & Grancini, 2021).

The perovskite-like material, $Cs_2TiBr_6$, has been considered a non-toxic alternative that is earth-abundant and biocompatible (Chen et al., 2018). However, because the material is new, there are limited comprehensive life cycle assessments of toxicology and environmental impact. Although titanium is considered a non-toxic metal, it can have negative health impacts when exposed to in high quantities or over long periods of time. It is currently used in pharmaceutical and dental settings, but it still has the potential to affect lung function and cause irritation of the skin or eyes. Some studies also suggest that it may be carcinogenic (Skocaj et al., 2011). Inhalation is suggested to be the most vulnerable entrance point of titanium to the human body. Animal studies have shown that the particles deposit in the lung, where they may cause chronic inflammation and tissue damage (Skocaj et al., 2011). Due to these potential consequences, occupational exposure should be controlled, and protective measures applied to protect workers involved with the synthesis and usage of this perovskite-like material (Skocaj et al., 2011).

Furthermore, titanium is sourced from several different developing countries, where mining operations could damage environments, traditions, and livelihoods. Cesium, another element involved in the synthesis of this perovskite-like material, is sourced most often from pollucite, a mineral found in high abundance in Zimbabwe. This could lead to similar exploitation and depletion of resources. The impacts of resource extraction and material

substitution on developing countries are explored later in this chapter and provide another concern for the implementation of a new technology such as $Cs_2TiBr_6$.

Overall, compared to alternative perovskite-like materials, $Cs_2TiBr_6$ is a less toxic option, which makes extraction and usage safer for those involved in the commodity chain. It is also cheaper and faster to make than silicone solar panels. However, work still must be done to make the process safer and more equitable for all parties involved.

### *a.3 Environmental racism*

Although solar energy sounds like a reasonable alternative to environmentally damaging fossil fuel usage, there are many aspects that do not fulfill the equity pillar of sustainability. Environmental racism is prominent in the solar industry, with the effects of climate change still disproportionately distributed. These transitions to renewable energy are essential for decarbonizing the world economy and mitigating global climate change, but technologies classified as renewable often have implications that jeopardize the wellbeing of those already most vulnerable to the impacts of the climate crisis (Levenda et al., 2021). The effects of our warming planet have a disproportionate impact on communities of color and low-income groups, so it is imperative to develop the most effective and equitable clean energy policies and programs as possible (Schultz, 2020).

The clean energy industry is lauded for providing economic opportunities, but these jobs are not allocated fairly across races and income levels. White and affluent communities get most of the jobs, while also gaining the clean air and financial benefits of utilizing the new technologies (Gearino, 2020). As shown in Figure 15, in 2019, only 7.7% of the solar workforce

was black. This is significantly less than the 13% of the entire American workforce that is black (Gearino, 2020).

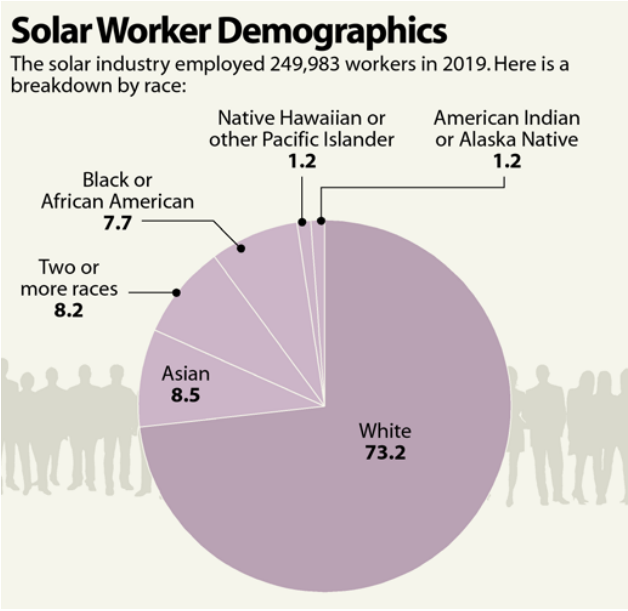


***Figure 15.*** *The demographics of workers in the solar industry in 2019 (Gearino, 2020).*

Even after accounting for income disparities and home ownership rates, residents of neighborhoods with black or Hispanic majorities are less likely to have rooftop solar (Gearino, 2020). Majority black neighborhoods also have higher levels of air pollution from industry and fossil fuel electricity than majority white neighborhoods (Gearino, 2020). If the benefits of this industry are mostly limited to people who already are in a position of privilege, this leads to justified resentment. In turn, this resentment can be exploited by industries that want to slow down the transition to clean energy, further hindering the progress of the clean energy movement (Gearino, 2020). For example, some utilities have sought help from NAACP chapters to oppose rooftop solar, based on the argument that the benefits of solar are going to mainly white and affluent households, shifting costs to everyone else (Gearino, 2020).

To better understand the work happening on the ground in relation to the distribution of green energy, I had a discussion with Judy Diamondstone, a member of Renewable Energy Worcester (RENEW). RENEW is "a Community Energy Cooperative run by Co-op Power members in Worcester County, MA to organize and advance the goals of energy justice and community resilience" (REWEW, n.d.). They are currently focused on community solar power,

and part of this initiative is understanding how renewable energy can be looked at through a social justice lens.

Judy discussed how the communities that currently have renewable energy are the ones that can afford to; they have the upfront capital, tax appetite to get subsidies, and good credit scores for loans. These are the people who can take advantage of new technologies and their benefits. This makes the cost of potential new solar panel technologies, like PSCs, even more important to understanding how they can be distributed more broadly. The communities that cannot afford to use this technology are stuck on fossil fuels, while rate structures change, and natural gas becomes more expensive. Figure 16 shows the rising prices of natural gas for residential consumers since 1985 (US EIA, n.d.).

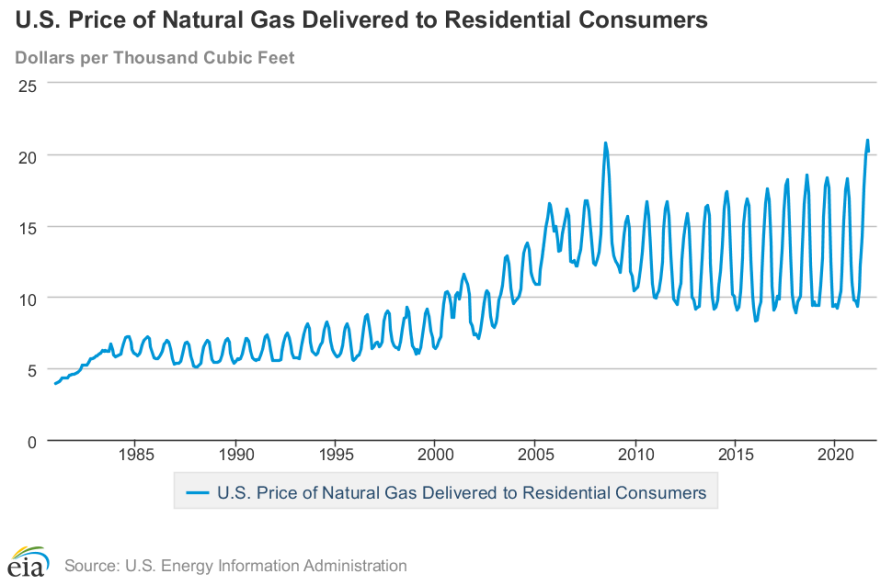


***Figure 16.*** *The price of natural gas delivered to residential consumers in the United States from 1985 to present (US EIA, n.d.).*

It is estimated that by 2036, half of the world's fossil fuel assets will be worthless under a net zero transition (Watts et al., 2021). The countries that are slow to decarbonize will suffer, but early movers will profit. This leaves people who can't afford new technologies paying for the expensive and failing natural gas infrastructure (Watts et al., 2021). Judy talked about how policies favor the people who already have the means to adopt the more expensive infrastructure, bringing equity to the forefront of the climate issue.

Judy discussed a lot of the local problems that are perpetuated by legislatures' inaction. In Worcester and the general Massachusetts area, we must first address the old buildings and infrastructure to allow for greater energy efficiency. Legislature must change at the state level to make this possible, due to legacy building codes in Massachusetts preventing implementation of requirements for new construction to get off gas infrastructure. It is also very costly to convert existing buildings already on gas infrastructure to all electric. In Worcester, the Green Worcester plan is to make city energy all renewable by 2030, which is possible through bulk buying. Worcester has also increased the proportion of renewable energy at no extra cost for citizens/residents, but people can still opt out and get electricity from National Grid.

There is still a long way to go before renewable energy, including solar panels, is made "sustainable." There are numerous public health implications involved with sourcing, distribution of solar technologies is currently inequitable, and changing the existing infrastructure is costly and time-consuming.

### b. Implications of Material Substitution

In the search for "green" technologies to combat the worsening climate crisis, researchers often opt to replace specific materials and processes that may be hazardous to the environment or human health. Material substitution has been used for centuries to reduce costs and enhance quality of new technologies, while also being used to avoid resource depletion while still making new advancements (Tilton, 1991). This has involved the introduction of new materials as well as improvements to old materials (Tilton, 1991). These substitutions can be made, in theory, to reduce ecosystem degradation and carbon emissions, or to improve public health. However, this substitution process also has the potential to result in the rapid depletion of a potentially scarce resource or increased extraction of other environmentally problematic materials (Graedel, 2002). These potential substitutes can also require a lot of time and money to develop, further depreciating their value despite possible environmental benefits (Graedel, 2002).

In one article, a researcher detailed a few different case studies related to this issue. One such case study was on the automobile catalytic converter. As early as the 1970's, it became clear that smog in urban areas was a byproduct of the emission of nitrogen oxides and hydrocarbons from automobile exhaust pipes (Graedel, 2002). In response, a two-stage platinum-

palladium catalytic converter was implemented to oxidize hydrocarbons to $CO_2$ and water, as well as to reduce the oxidation of nitrogen to dinitrogen (Graedel, 2002). In less than a decade, this led to a doubling of platinum production, which was only possible to control due to the slow adoption of catalytic converters. With transference of this technology to other countries coupled with a demand for platinum in additional new products, the platinum supply could be severely strained (Graedel, 2002). Although this change helped to reduce smog levels in urban areas, it put pressure on resource supplies and illustrates the potentially damaging implications of material substitution.

Another example from the same study is ammunition. For several hundred years, lead was used in shotgun ammunition. This led to lead deposition on fields and woodlands and in lakes and marshes, poisoning local birds and other organisms (Graedal, 2002). Due to the impacts of lead ammunition on ecosystems, there was a push to substitute the material with something less toxic, like bismuth, steel, tin, and tungsten. However, none of these materials were ideal for substitution for a variety of reasons. Steel, which is one of Earth's most abundant elements, is lower in density. Tin and tungsten are closer in density to lead, but neither are as similar to it as bismuth. Thus, the use of bismuth was pursued as a replacement. Environmental benefits and similarities aside, if used universally in place of lead, the entire global supply of bismuth would be exhausted in two or three years (Graedal, 2002). The local environmental benefits are great, but the substitution is unsustainable in the long-term.

The implications of material substitution are necessary to consider when attempting to substitute titanium and cesium in place of volatile organic ions and toxic heavy metals. A main concern is the effect of resource mining on local communities, which will be discussed later in the chapter. Titanium, for example, is mined from Kenya, where communities are still experiencing alarming socio-economic conditions despite the billion-dollar titanium mining project occurring in their backyards (Business & Human Rights Resource Centre, 2017). There are also dire environmental and human health impacts on surrounding communities caused by industrial mining operations, particularly in developing African countries (Leuenberger et al., 2021).

### c. Implications of resource extraction

As with material substitution, the extraction of resources for use in industrial applications can have detrimental effects that must be considered before widespread implementation of a new technology. This consideration is necessary not just for new perovskite materials, but for existing solar panel technologies as well. A main concern is the implication that resource extraction has on human rights in developing countries due to their resource rich land. Two prime examples of the impacts of resource extraction on developing countries are Congo's cobalt rush and Guinea's bauxite mining.

### *c.1 Guinea's bauxite mining*

Guinea, located on Africa's west coast, possesses the world's largest reserves of bauxite, which is used to make aluminum (AfricaNews, 2021). This country holds around a quarter of the global total of bauxite yet remains one of the world's poorest countries (AfricaNews, 2021; Wormington, 2018). Guinea is the top global exporter of bauxite, with China as the biggest importer and producer of aluminum. A large proportion of the aluminum is used in car and airplane parts as well as in consumer products like beverage cans and tin foil (Wormington, 2018). Because of the concentration of bauxite in this one location, the production chain is heavily dependent on the local mines, leading to soaring prices and shortages along the commodity chain when major events happen in the source country, such as a coup (AfricaNews, 2021).

Aside from increased dependence on these locations, there are major human rights impacts that stem from the mining operations. Like titanium mining in Kenya, there is very little benefit for the communities themselves. On the contrary, these operations can be detrimental to livelihoods and human health. The Boke region of Guinea has been the center of the mining operation's recent growth, with open-sky bauxite quarries, use of heavy machinery and dynamite, mining roads and railroads through rural communities, and industrial ports within mangroves, paddy fields, and local fishing ports (Wormington, 2018). The mines provide tax revenue for the government, jobs, and large profits for mining companies and shareholders. However, there are also consequences for rural communities that live close to mining operations, where companies take advantage of the ambiguity of land protection laws. This has led to damage to water sources, air quality concerns, and loss of land due to lack of government transparency and exploitative mining companies (Wormington, 2018). Loss of local land is

compounded by damage caused to remaining farmland, such as dust on the fields. With dirty water and altered hydrology, there is less access to streams and springs previously used as water sources. Despite this, there is increased demand for water due to population migration to mining communities. As a result, women must walk longer distances or wait longer periods of time to obtain alternatively sourced water (Wormington, 2018). Additionally, the poor air quality produced by mining and transport has smothered fields and has led to both public health and environmental concerns. The dust gets everywhere, even into food, and exposure to any fine particle dust can cause, trigger, or exacerbate respiratory and cardiovascular diseases (Wormington, 2018).

Because of these inadequate local services, riots are occurring in protest of the way that mining has upended the lives and livelihoods of local rural communities (Wormington, 2018). The lack of government transparency has prolonged these problems, with no publication of environmental and social impact assessment, monitoring reports, or public data. Without a way to hold companies accountable for neglecting human rights, the issue will not rectify itself. There must be more effort made to protect local resources, such as clean water supplies, as well as better monitoring of air quality. There is also a need for mining companies to offer forms of support along with their current financial payments, as the compensation provided is often difficult to use to provide sustainable sources of long-term income (Wormington, 2018). Despite how lucrative the bauxite mining industry is for companies and stakeholders, there is immense damage occurring to the local developing communities' environments and livelihoods.

### *c.2 Congo's cobalt rush*

A similar set of human right violations has been occurring during Congo's cobalt rush. The Democratic Republic of the Congo (DRC) sits atop almost half of the world's known supply of heterogenite, which can be refined into cobalt for use in lithium-ion batteries (Niarchos, 2021). These batteries are in high demand for electronics, and cobalt has even been considered as an alternative to iodine for solar panel production due to its greater earth abundance, with its substitution being touted as a "sustainable" step forward (Universität Basel, 2013). The heterogenite was first found in Kolwezi, a once remote area that is now a city with half a million residents (Niarchos, 2021). When the cobalt was discovered, people began hoarding the supplies they found and digging their own plots out of desperation and desire for profit (Niarchos, 2021).

Despite the attempts made by locals to profit from their land, there were detrimental effects on both public health and the environment that arose as a result. Near the mines, there were teen boys working perilous shifts, prostitution of women and girls, women washing raw material, and people performing sinister rituals to "improve luck" in the mines (Niarchos, 2021). The raw material that women were often working with is full of toxic metals and sometimes mildly radioactive. When pregnant women are exposed to these heavy metals, it can increase the chances of stillbirth or children with birth defects. The metal concentrations are among the highest ever reported for pregnant women (Niarchos, 2021). There are also links between fathers who worked with mining chemicals and fetal abnormalities (Niarchos, 2021).

Aside from the health impacts on the workers, there are a variety of human rights issues that have stemmed from the operations. With mineral riches in a poor country, there is a heightened temptation for politicians and officials to steal and cheat for their own gain. In the Chinese-run mines, there were often racist and harsh conditions, with China's influence sometimes considered a "new form of colonialism" (Niarchos, 2021). Children worked in the mines, and increased drug and alcohol use became prevalent amongst the miners (Niarchos, 2021). With little regulation or support from the government, this has run rampant and severely impacted the livelihoods of those in these communities.

### d. $Cs_2TiBr_6$

Like other resources mined globally, the implications of cesium and titanium mining for growth of $Cs_2TiBr_6$must be considered before there is mass production of PSCs. Cesium is rare globally, and China currently has a monopoly on it. It has been listed as a critical metal in Australia and America, meaning that it is deemed crucial for future technological advancement (Trueman, 2021). Cesium is worth up to twice the price of gold, and the three producing mines in the world are all controlled by China (OilPrice.com, 2020). These mines are the Tanco mine in Manitoba, the Bitika mine in Zimbabwe, and the Sinclair mine in Australia (OilPrice.com, 2020). The United States has low-grade deposits of cesium ore in South Dakota and Maine, which are currently not economical to mine. As a result, the U.S. imports 100% of the cesium it uses (*Cesium,* n.d.). With Chinese control, there may be potential for the employment of destructive, unregulated practices like those in the Chinese run mines in Congo. Cesium is also the most electropositive of all stable elements in the periodic table and ignites spontaneously when in

contact with air (OilPrice.com, 2020). It is extremely reactive and can burn the skin, so it must be handled with care (*Cesium*, n.d.). This may create safety concerns in the mines. However, this electropositivity also allows it to form very stable compounds, which could be of particular interest in the case of solar panels (Trueman, 2021).

Despite the sourcing concerns, there are new possible locations for mining operations, some of the more notable sites found in Canada and Australia (OilPrice.com, 2020). Avalon Advanced Minerals is the only near term and potential producer of pollucite in North America, from its Lilypad Cesium Project in Northwestern Ontario (Trueman, 2021). Additionally, there are already cesium compounds in use that are eco-friendly and can be readily recycled. For example, cesium-formate is used in high pressure, high temperature, deep oil and gas well-drilling as a coolant and lubricant. It is also well-known for medical applications (Trueman, 2021).

There are also concerns to be addressed in relation to the mining of titanium. Titanium is also considered a critical mineral, particularly in applications that serve aerospace, defense, and energy technologies (Virginia Energy, n.d.). There are numerous properties that make titanium valuable for use in several different applications. These include its relative nontoxicity and low reactivity, efficient strength to weight ratio, corrosion resistance, and high melting point (Geoscience Australia, 2018; Seagle, n.d.; Virginia Energy, n.d.). However, despite the abundance of titanium ores, the high reactivity of the metal with oxygen, nitrogen, and hydrogen in the air at elevated temperatures leads to costly production and fabrication processes (Seagle, n.d.; Geoscience Australia, 2018). These costly processes also have environmental consequences, such as destruction of ecosystems in mining areas. Some mines, like those in coastal Western Australia, have methods of rehabilitation for revegetation and topsoil replacement, which is necessary for obtaining titanium sustainably (Geoscience Australia, 2018). Additionally, the U.S. does not maintain a supply of titanium in the National Defense Stockpile and is 91% reliant on imports from Japan, Kazakhstan, Ukraine, China, and Russia. In the United States, titanium is mined in smaller amounts in Nevada, Utah, and Virginia (Virginia Energy, n.d.).

Kenya's large titanium deposits found on the coast makes it a location of interest in the titanium mining industry. In 2002, they accounted for 40% of the world's known unexploited titanium reserves and are claimed to be worth trillions of dollars (Abuodha, 2002). This could be

a significant economic opportunity for Kenya. However, it could also significantly damage surrounding communities' environments and livelihoods. A common effect of mining is the displacement of a huge population of indigenous landowners. Stemming from this are issues with landowner compensation, particularly during involuntary resettlement and population movement (Abuodha, 2002). Additionally, beach mining has the potential to significantly alter the system of sea currents and sediment transport patterns, on top of the pollution and extensive ecosystem disruption (Abuodha, 2002). Like Congo and Guinea, the loss of this land and destruction of marine resources can lead to a loss of social dynamics and cultural cohesion. It is common for mine operators to clash with the interests and wishes of native communities (Abuodha, 2002). There are also radioactivity dangers associated with titanium mining, usually from zircon and monazite, which are naturally present in deposits with titanium dioxide. For example, in Australia, 10% of mineral deposits are heavy minerals, with 1-3% of those heavy minerals containing monazite. This in turn contains 5-7% radioactive thorium and 0.1-0.3% uranium (Abuodha, 2002). Kenya has an estimated 20% heavy mineral deposits, making the associated risks even more significant.

Now that the titanium mining industry is booming in Kenya, communities have still benefited very little despite the billion-dollar business operating in their backyards (Business & Human Rights Resource Centre, 2017). With all the evidence of impacts of mining operations on developing countries, the effects of mining resources for solar panels, both conventional and perovskite-based, is of utmost importance. The health and safety implications of mining these materials is also important to take into consideration to avoid endangering public health throughout all components of the commodity chain. These considerations are all necessary to make sure the new technologies are not just green, but sustainable.

# II. Methodology

## 1. Sample Synthesis

Samples are grown and prepared by Emma Pellerin, a member of Ron Grimm's chemistry lab group. Cesium titanium bromide, $Cs_2TiBr_6$, is made through a synthesis of cesium bromide, CsBr, and titanium bromide, $TiBr_4$, as described in Mendes et al., 2020. It is made as a high

temperature melt with no other solvents involved in the process. Once the material is synthesized the sample is placed on a quartz round held by an aluminum plate and sealed by placing a gasket around the sample and then another aluminum plate and quartz round. The gasket screws are then carefully placed and tightened, taking care to do this slowly so that there are no fractures in the quartz, exposing the sample to air and risking oxidation. At this point, the sample is ready for data collection. More information about this process is given in Appendix A, which details Emma Pellerin's single crystal synthesis process. An example of the PL cells we use for data collection containing a thin film sample is shown in Figure 17.

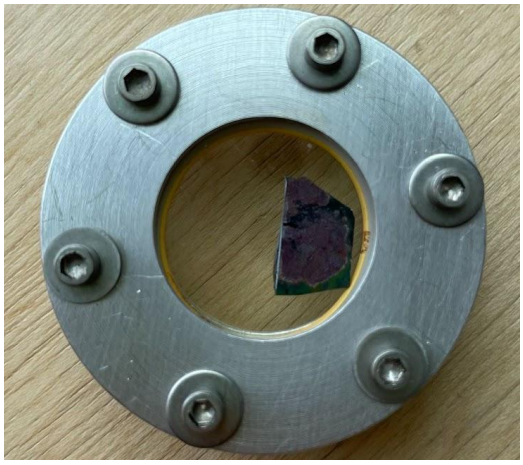

***Figure 17.*** *Thin film sample sealed between quartz rounds.*

## 2. Visual Analysis of Sample

The first step in our experimentation involved visual examination of the samples. Its pronounced red color, corresponding to the band gap in the red range of visible light (~ 1.8 eV) indicated that the sample has not oxidized. Striations and terraces on single crystals indicated steps on the surface.

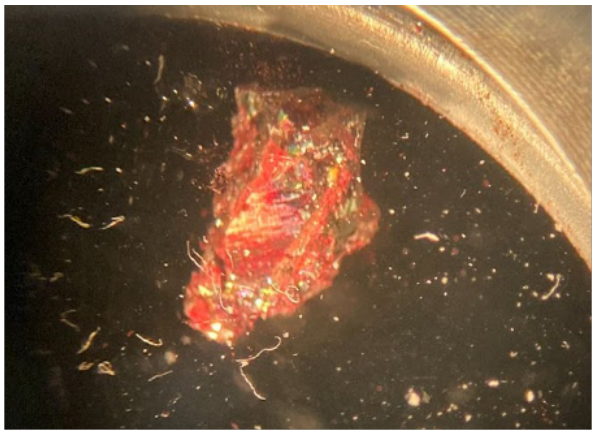

***Figure 18.*** *One half of a cleaved single crystal sample sealed between two quartz rounds, observed through a stereoscope.*

We first focused our data collection on portions of the crystals with more striations, like the center of the crystal shown above in Figure 18. This figure represents an image of one of our samples under a stereoscope. The striations indicate where this sample was cleaved and, in our experience, led to higher optical emission and better signal to noise ratio in our data.

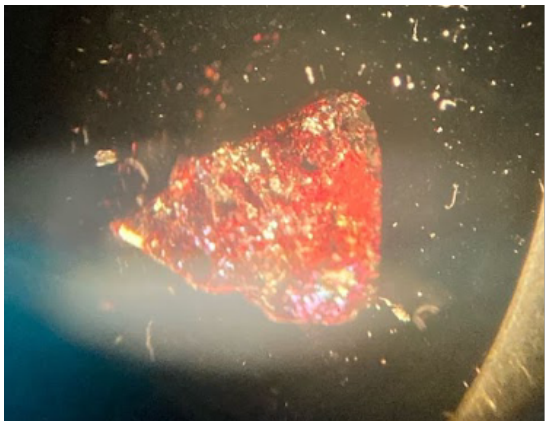

***Figure 19.*** *Second half of a cleaved single crystal sample sealed between two quartz rounds, observed through a stereoscope.*

The crystal shown above in Figure 19 has a variety of different textures; the thick right side of the crystal is smooth, whereas the thin left side of the crystal is more terraced. These are areas of interest for data collection to see if the topology of the crystal influences the signal and data obtained from PL measurements.

In both Figure 18 and Figure 19 the crystals appear to have a reddish coloration, indicating that these samples have not yet oxidized. However, in Figure 20, there is evidence of oxidation along the right side of the thin film sample, indicated by a yellowish coloration. This

was likely due to fractures in the quartz rounds caused by the sealing process, allowing air to reach the sample and compromise it.

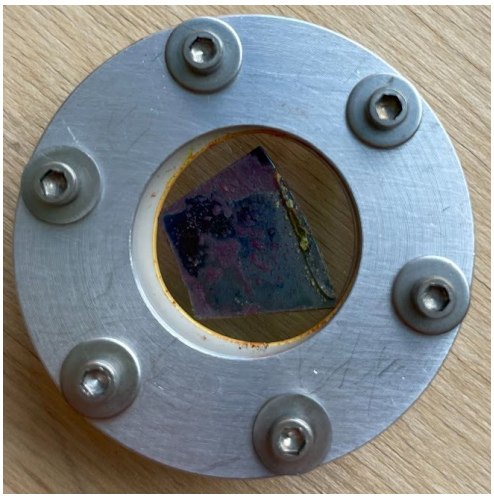

***Figure 20**. Thin film sample sealed between quartz rounds with visible oxidation.*

## 3. Experimental procedure

### a. Photoluminescence Set-Up

For data collection, we used a micro-PL system consisting of Horiba MicOS microscopy attachment, iHR550 imaging spectrometer, Synapse CCD detector for spectrally resolved, time-integrated measurements, and Aurea TCSPC system for time-resolved measurements (Figure 21). A pulsed 485 nm laser with the pulse duration of ~ 50 ps and variable repetition rate (1kHz-20 MHz) was used as a source of optical excitation.

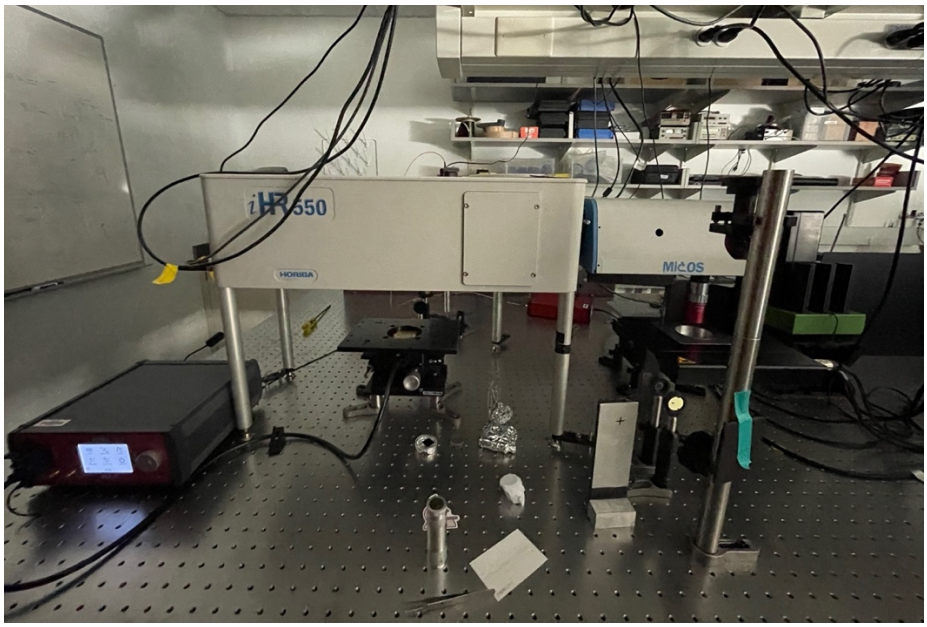


***Figure 21.*** *PL setup in WPI's Ultrafast THz and Optical Spectroscopy Lab.*

The room was kept dark during data collection, bar the light from the computer, so that there was minimal interference with spectra generation.

### b. Program and Data Collection

For the measurements, the sample was positioned under the 50X Mitutoyo long focal length optical objective. The objective focused the excitation laser to a ~ 2 μm spot on the sample surface and collected the emitted light. A long-pass optical filter (Thorlabs FEL 500) placed before the spectrometer entrance slit blocked scattered excitation laser light from impacting the measurements. Optical camera integrated into MicOS system allowed us to observe the surface and select specific locations for the measurements. As mentioned earlier, this was chosen with a variety of factors considered, such as surface texture and color. The fluence of the excitation, defined as energy of the excitation laser pulse divided by the area of the sample illuminated, was controlled by using the "Tuning" function of the laser. For all the reported measurements, fluence values ranged between 470 $\mu J/cm^2$ and 290 $\mu J/cm^2$. We have measured spectra in multiple sample locations to minimize the effects of possible chemical degradation. As the emission efficiency is typically quite low due, presumably, to the indirect gap nature of our samples, we improved signal to noise ratio in time-integrated PL spectra by averaging over multiple spectral acquisitions. We found that 20 accumulations provided the optimal balance

between signal/noise ratio and total experiment time and surface degradation due to focused laser exposure.

For recording PL decays, Aurea avalanche photodiode (APD) was used instead of a CCD detector. It is mounted on a different exit slit of the spectrometer, and a spectrally resolved signal can be directed to the APD using a software-controlled exit mirror. In carrying out TCSPC measurements, it was important to consider the excitation repetition rate. High repetition rates of the pulsed source increased the count rates and improved the signal-to-noise ratio. However, the time between each excitation still had to be longer than the relaxation time of the carrier to the ground state (De los Reyes, 2015). Furthermore, PL count rate needs to be less than 5% of the laser repletion rate so that the probability of two photons emitted by the sample following a single laser pulse was low. This avoids so-called 'pulse pile-up', an artifact that results in the radiative recombination rate appearing higher than it is. In our measurements, we could change the repetition rate of the laser from 1 kHz to 20 MHz. We found that 10 MHz repetition rate yielded the best signal to noise ratio, and it was used in all measurements reported below.

## 4. Analysis Instruments

Once we collected the data, we used Origin Lab to analyze it and fit the decays and spectra. We first imported all the data as multiple ASCII files, and converted the wavelengths to energy in units of electron volts (eV) by using a factor of

$$\frac{1239.8}{\lambda} \qquad (1)$$

This data was then generated into a line plot and analyzed using the peaks and baseline multiple peak fit. The data from all three tunings at a given wavelength were overlaid for comparison. From this data we determined locations of defect states and direct or indirect bandgaps to better understand the properties of the material.

Next, we used the data from our histograms to generate a decay fit. We first made sure the histogram was shifted to start at 0, then we analyzed it by fitting it to a nonlinear curve. To determine what order exponential to use if unsure, we double clicked on the y-axis and chose the scale tab to determine the number of slopes through use of a logarithmic scale. This number was then applied as the order exponential. After this determination, the scale must be returned to linear. The fit equations most frequently used in our analysis were ExpDec1 (2) and ExpDec2 (3), as shown below.

$$y = y_0 + A_1 e^{-x/t_1} \quad (2)$$

$$y = y_0 + A_1 e^{-x/t_1} + A_{12} e^{-x/t_2} \quad (3)$$

This was done on decay information from three fluences (at one common peak on a particular sample), overlaid onto a single graph.

# III. Results

## 1. Thin Film Samples

Prior to data collection, pictures were taken of each sample to document oxidation locations and possible points of interest. Samples A and B are depicted, respectively, in Figure 22. For data collection, we obtained spectra and decays for one point on sample A, and two points on sample B. Sample B had a deeper red color than sample A.

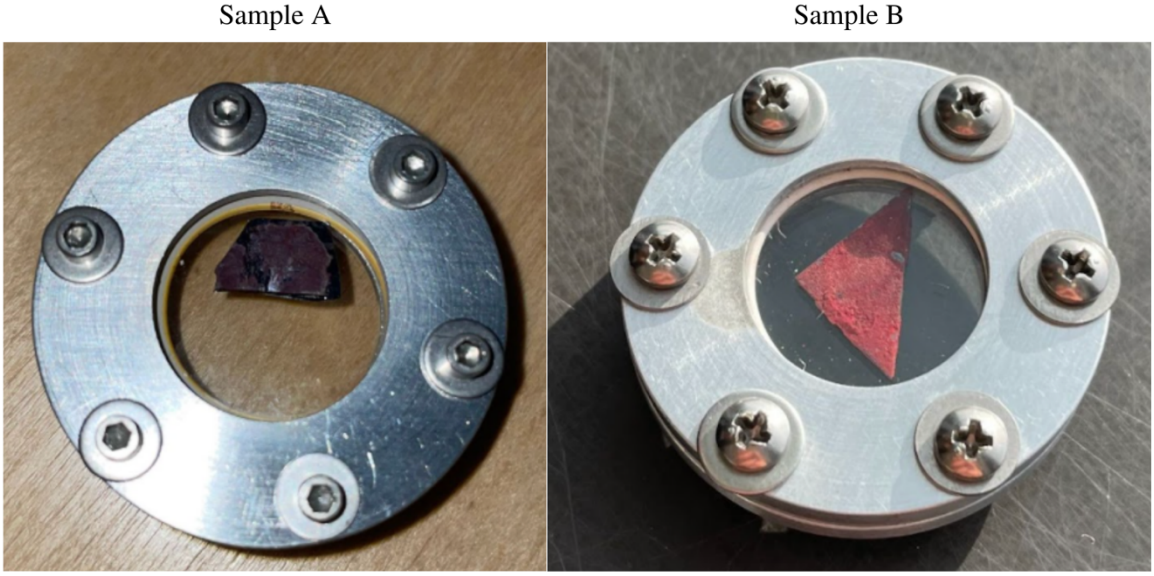


***Figure 22.*** *Thin film samples A and B, respectively, photographed prior to data collection.*

To help determine relevant optical properties of the material, we generated spectra for various points on the thin film samples. For each sample/data point, we collected the spectra for three different fluences. Figure 23 depicts the spectra generated for sample B1.

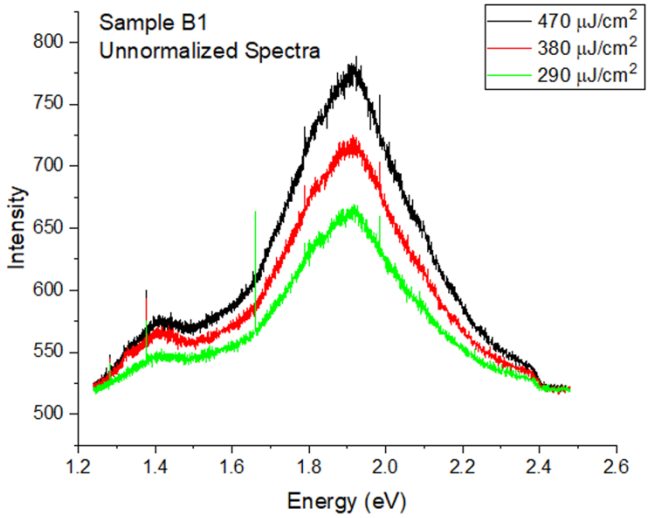


***Figure 23.*** *Unnormalized spectra taken from the first point of data collection on Sample B (B1), at three fluences.*

As the fluence increases, the intensity of the generated spectra increases proportionally. The spectra were normalized for ease of comparison between the samples. The normalized spectra for each data point are shown below in Figure 24. The spectra for all three data points were collected at a laser frequency of 10 MHz over a period of 20 accumulations.

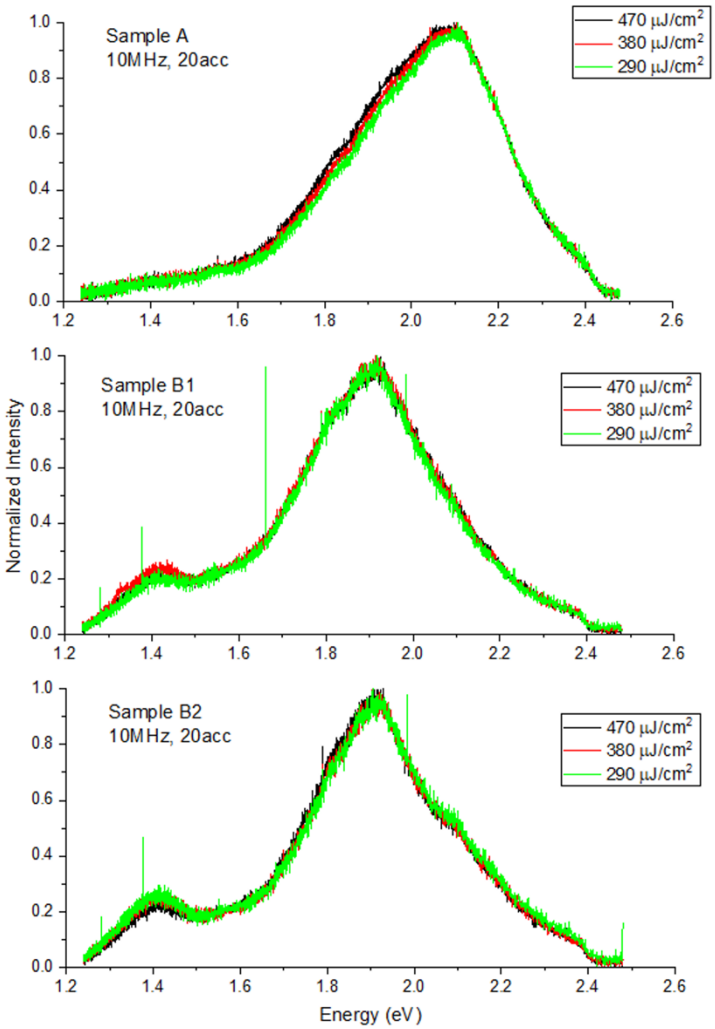


***Figure 24.*** *Normalized intensity (counts) versus energy (eV) of three thin film set of data, taken at 10 MHz and 20 accumulations at three fluences.*

We find that increasing the fluence increases the overall intensity but does not change the spectral shape. We also find that spectra vary somewhat from point to point, and between the two samples. Samples B1 and B2 both have a peak at around 1.9 eV, whereas sample A exhibits a peak at around 2.1 eV. The expected indirect bandgap of this material is about 1.85 eV, as shown in *Electronic structure of Cs2TiBr6 from UV-visible spectroscopy,* Figure 10.

To supplement our analysis of the emission patterns of the samples, we also generated decays to compare time constants and related carrier lifetimes. The decays exhibited similar patterns to the spectra, where increasing the fluence altered the intensity of the decays proportionally. Figure 25 shows the normalized decays for all three fluence outputs on sample B1, where the shape of the decay is relatively unaltered as the fluence is increased.

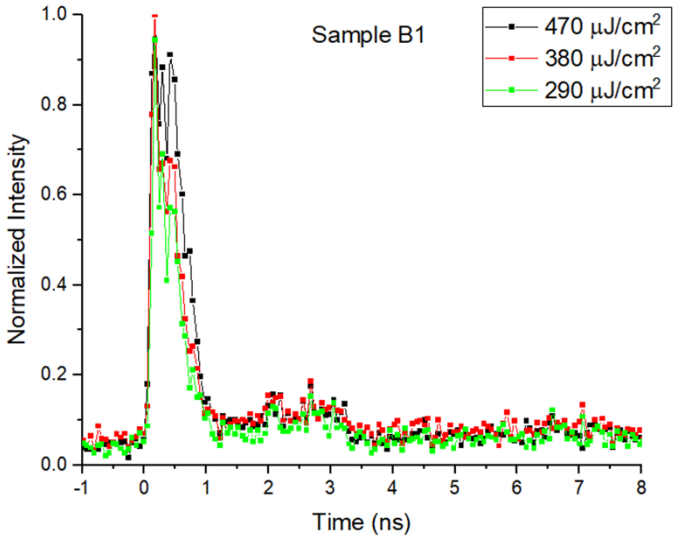


***Figure 25.*** *Decay histograms from Sample B1 taken at three fluences at the peak of PL spectrum (1.9 eV).*

For the three data points collected, we generated normalized decays at only one fluence, 290 $\mu J/cm^2$, as the shape of the decays does not differ with alteration of the fluence. Figure 26 shows the normalized decays for the three thin film data points, fitted exponentially with their time constants represented.

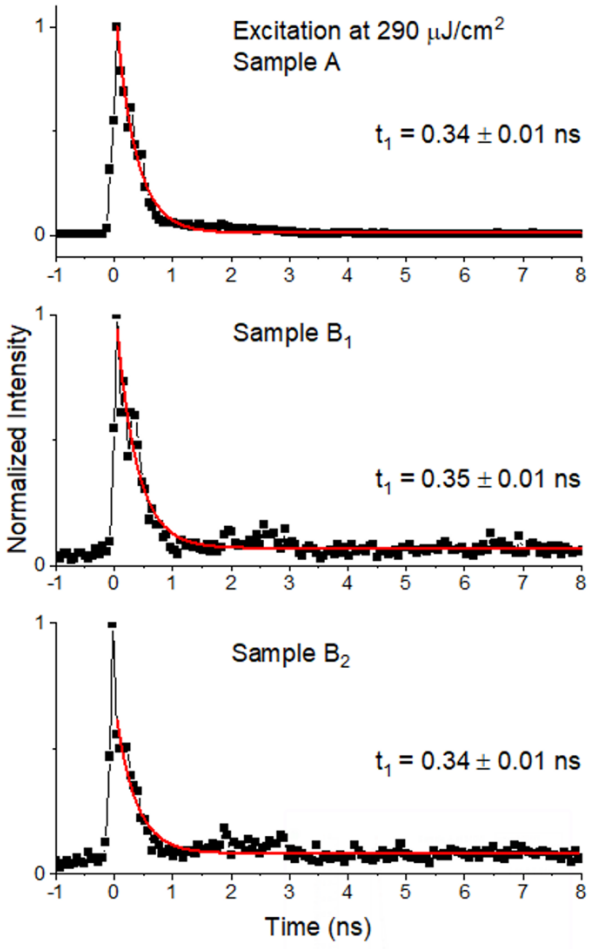


***Figure 26.*** *Decay histograms taken at 290 μJ/cm² from Sample A, Sample B1 and Sample B2, fitted with ExpDec1, showing respective time constants of decay.*

Over the three data points, the time constants are experimentally equivalent, differing only by the uncertainties.

## 2. Single Crystal Samples

We followed a similar procedure for analysis of the single crystal samples. We first took pictures of the samples prior to data collection for possible comparison. Samples C and D are depicted, respectively, in Figure 27. For data collection, we obtained spectra and decays for one point on sample C, and two points on sample D. The data from sample C was taken from the top crystal. Visually, the samples had similar colors and points of interest, with some variations in surface texture and shape.

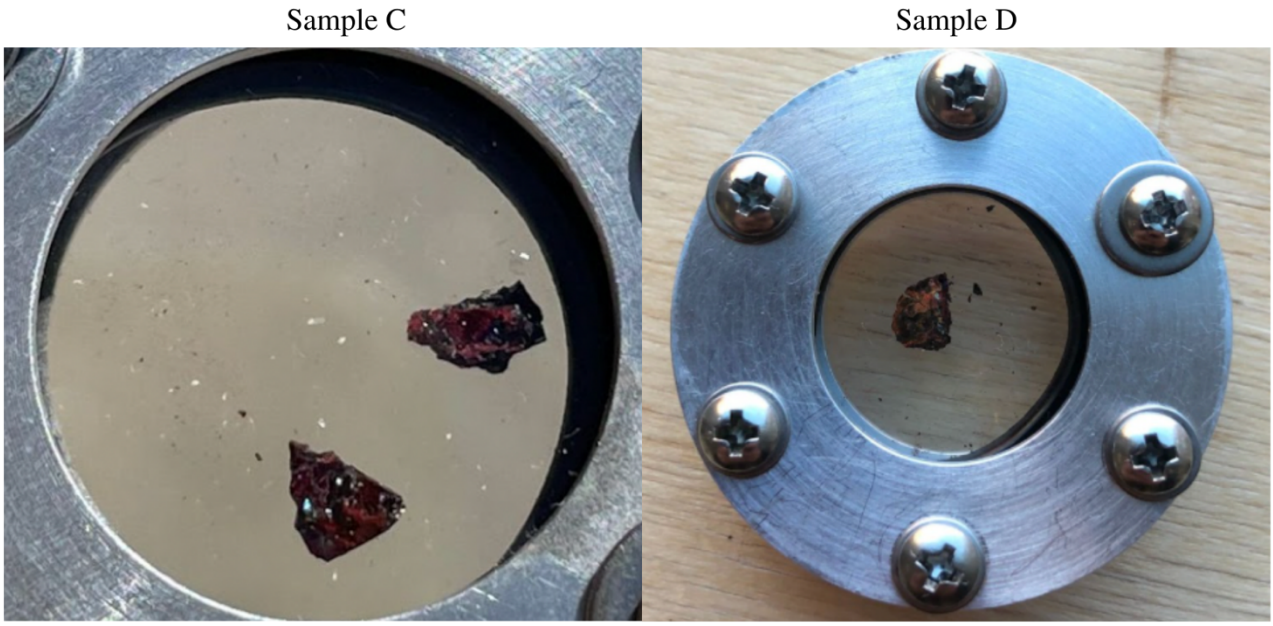


***Figure 27.*** *Single crystal samples C and D, respectively, photographed before data collection.*

As with the thin film samples, we collected data at each point at three different fluences. The spectra generated at each fluence for sample D1 are shown in Figure 28.

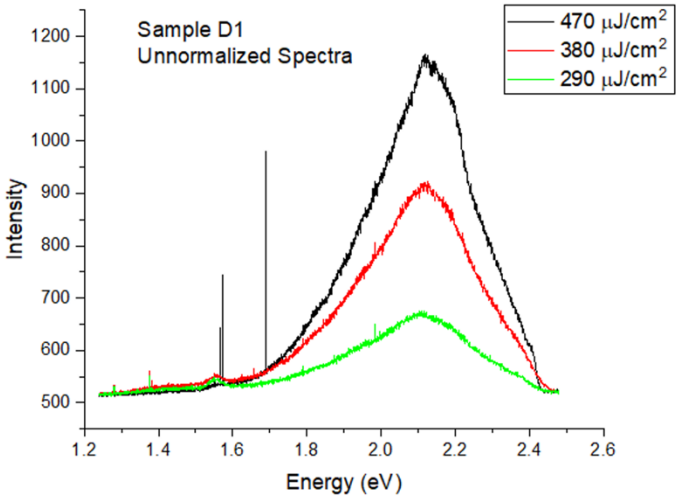


***Figure 28.*** *Unnormalized spectra taken from the first point of data collection on Sample D at three fluences.*

For each of the three data points of interest, we generated normalized spectra to visualize the differences and similarities between samples. Figure 29 depicts these normalized spectra. The

spectra for all three data points were collected at a laser frequency of 10 MHz over a period of 20 accumulations.

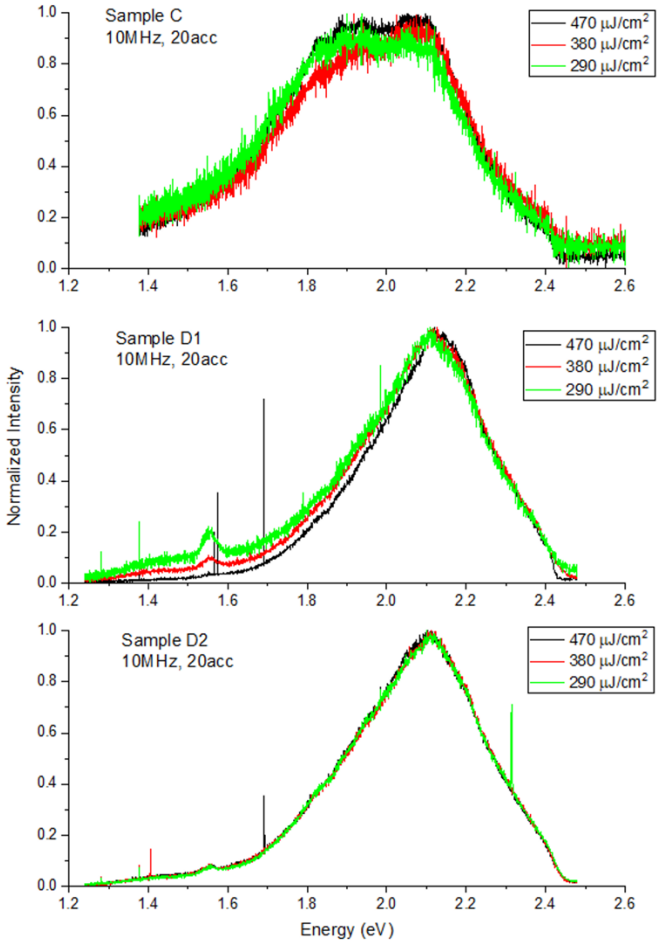


***Figure 29.*** *Normalized intensity (counts) versus energy (eV) of three single crystal sets of data, taken at 10 MHz and 20 accumulations at three fluences.*

For these samples, there is a little variation in shape between the different fluences. Sample D2 exhibits the relationship between fluences that was to be expected from our analysis of the relationship between intensity and fluence. There are also different characteristics between sample C's spectra and the spectra from the two points on sample D. Samples D1 and D2 have similar shapes. All three samples exhibit peak intensities at around 2.1 eV; however, sample C has a second peak at around 1.9 eV. These are higher than the band gaps determined through previous experimentation, as discussed in Section 1.

We have also explored the effects of oxidation on the PL spectra. After the initial data collection for sample C, we left the sample in the lab for a week and a half at ambient conditions. It remained sealed but was not returned to the glovebox. Figure 30 shows a side-by-side of the original sample and the oxidized sample. The original sample is on the left-hand side of the figure, and the oxidized sample is on the right-hand side.

Sample C - Original | Sample C - Oxidized

***Figure 30.*** *Single crystal sample C photographed at original time of data collection and after a week and a half of being left out of the glove box, respectively.*

For both data collection periods, we obtained spectra at a point on the top crystal. Here, we can observe that the sample appeared to have been completely oxidized; little to no red remained after a week and a half had passed.

Below, Figure 31 compares the original and normalized spectra for sample C fresh out of the glovebox and for sample C after a week and a half.

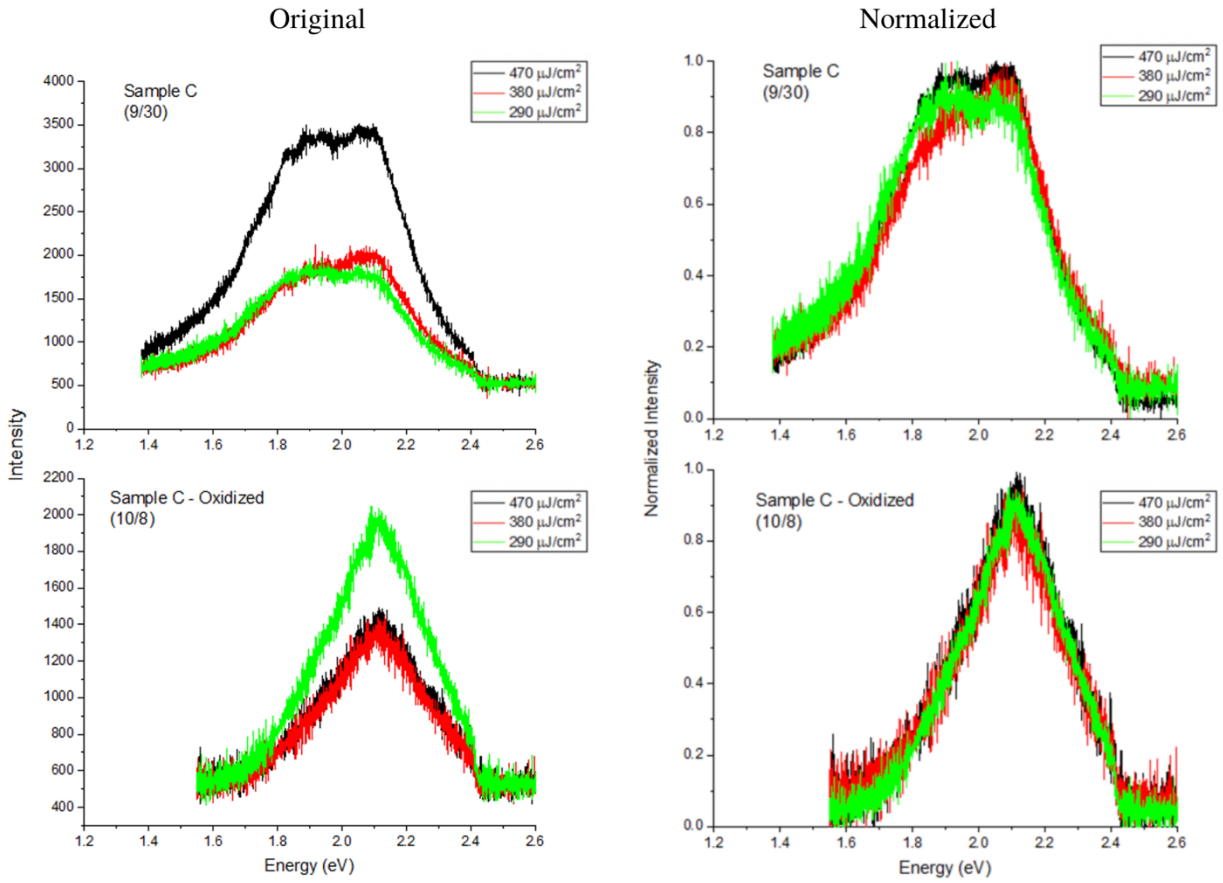


***Figure 31.*** *Original spectra (left) and normalized spectra (right) for sample C, before (top) and after (bottom) being left out of the glovebox and being allowed to oxidize for a week and a half.*

Here, we observed a change in general shape of the spectra, with only one peak at 2.1 eV observed for the oxidized sample. This shape mirrors the shapes of the spectra for the two data points on sample D, given previously in Figure 29. There are also unexpected differences in the fluence/intensity relationship that do not follow from the relationship obtained from sample D in Figure 28. The original sample has the same emission intensity at 380 μJ/cm$^2$ and 290 μJ/cm$^2$, instead of decreasing proportionally as expected. Additionally, the oxidized sample has the highest intensity at 290 μJ/cm$^2$ rather than at 470 μJ/cm$^2$, and the other two fluences generated similar intensities. We can also observe that the general magnitude of intensities decreased after oxidation occurred. We do not have decays for the oxidized sample, as we were unable to generate any sufficient data.

As with the thin film samples, we also generated decays to compare time constants and related carrier lifetimes. Figure 32 shows the normalized decays for all three fluences on sample D1, where the shape of the decay is relatively unaltered as the fluence is increased despite the increased intensities at higher fluences.

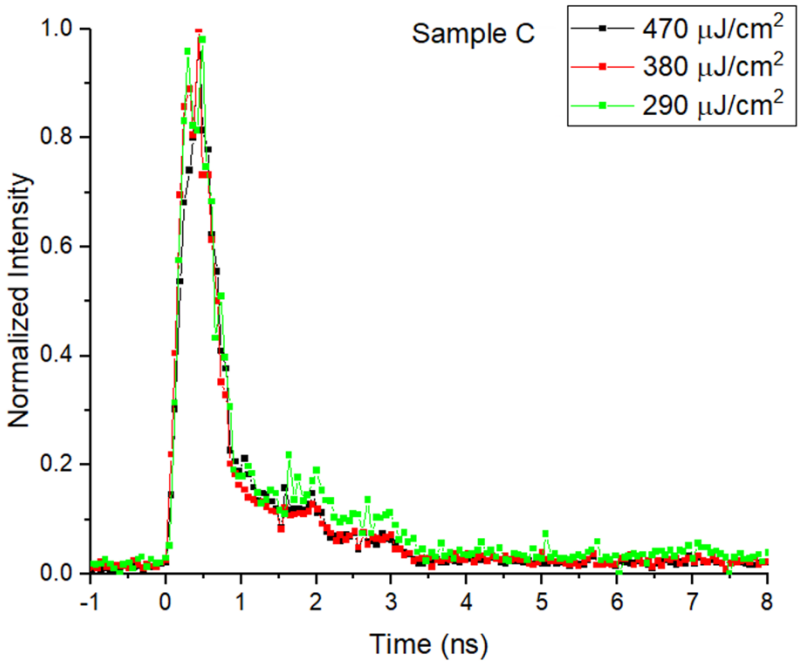


***Figure 32.*** *Decay histograms from point one on sample D taken at three fluences.*

For the three data points collected, we generated normalized decays at only one fluence, 470 μJ/cm$^2$, as the shape of the decays does not differ with alteration of the fluence. This fluence was chosen due to its decays exhibiting the lowest amount of noise. Figure 33 shows the normalized decays for the three single crystal data points, fitted exponentially with their time constants represented.

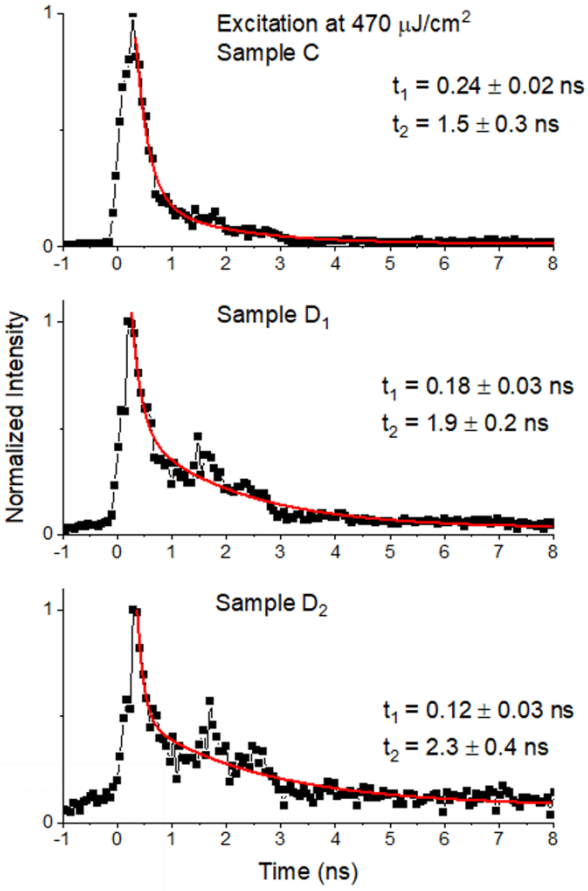


***Figure 33.*** *Decay histograms taken at 470 μJ/cm² from Sample C and two points of Sample D fitted with ExpDec2, showing respective time constants of decay.*

Over the three data points, the fits for the decays had two time constants. Their time constants are very similar, differing only slightly when uncertainties are accounted for.

## 3. Comparing Thin Film and Single Crystal Data

To understand potential applications and how our data compares to expected values, we compared the data obtained from thin film samples to the data obtained from single crystal samples. In Figure 34 we show the normalized photoluminescence intensity versus energy for both a single crystal sample (orange) and a thin film sample (purple).

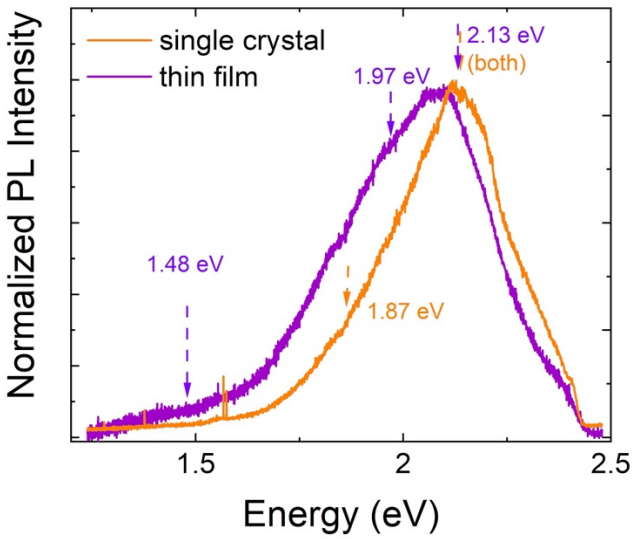


***Figure 34.*** *Normalized PL intensity (counts) versus energy (eV) of a single crystal sample (orange) and a thin film sample (purple), pointing out the distinct peaks on each spectrum.*

Both single crystal and film samples exhibit broad PL that can be deconvolved into multiple peaks (2.13 eV and 1.87 eV for a single crystal, and 2.13 eV, 1.97 eV and 1.48 eV for the thin film). The most prominent occurs at approximately 2.13eV for both samples, which is significantly higher than the expected band gap emissions. The indirect band gap emission was expected to occur at approximately 1.76 eV for the single crystal sample, and 1.85 eV for the thin film sample. Direct band gap emissions for single crystal and thin film sample $Cs_2TiBr_6$ are, respectively, 1.86 eV and 1.95 eV. Below in Figure 35, we have included a comparison of the UV-Vis data with the spectra generated for both a thin film sample and a single crystal sample. The UV-Vis data was not obtained from the same samples that the spectra were generated from. Thin film sample B1 is shown on the upper left-hand side of the image, and single crystal sample D2 is shown on the upper right-hand side of the image.

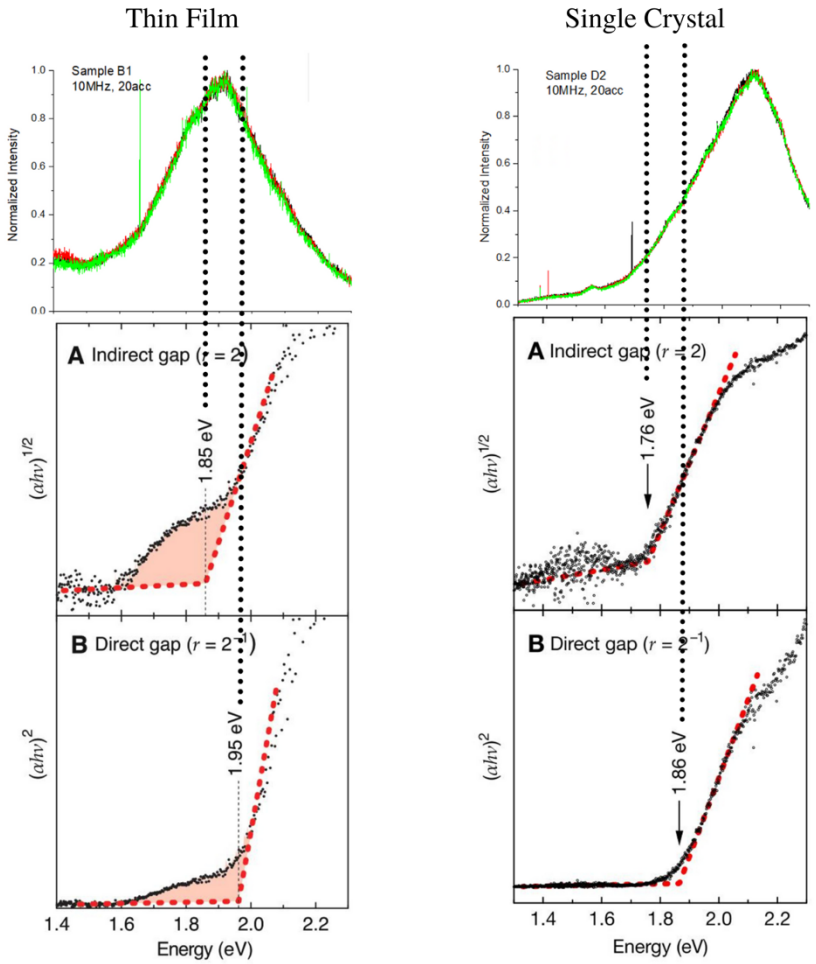


***Figure 35.*** *Thin film (left) and single crystal (right) spectra at three fluences compared to UV-Vis data taken from a thin film and single crystal sample, respectively. The samples used for UV-Vis were not the same as those used to collect spectra data.*

Here, we observe that the thin film spectra have a peak that corresponds closely with the expected indirect bandgap. The peak is slightly higher than the indirect bandgap, and lower than the direct bandgap. Conversely, the single crystal spectra do not have a peak that corresponds with either bandgap; the peak is significantly higher than expected. Even if we had used sample C as a basis for comparison with the UV-Vis data, the first of the two peaks at 1.9 eV are still greater than the expected indirect bandgap of 1.76 eV.

To determine any differences and similarities between the single crystal and thin film spectra, we placed the normalized spectra for the different samples side-by-side for comparison of shape. These are shown in Figure 36.

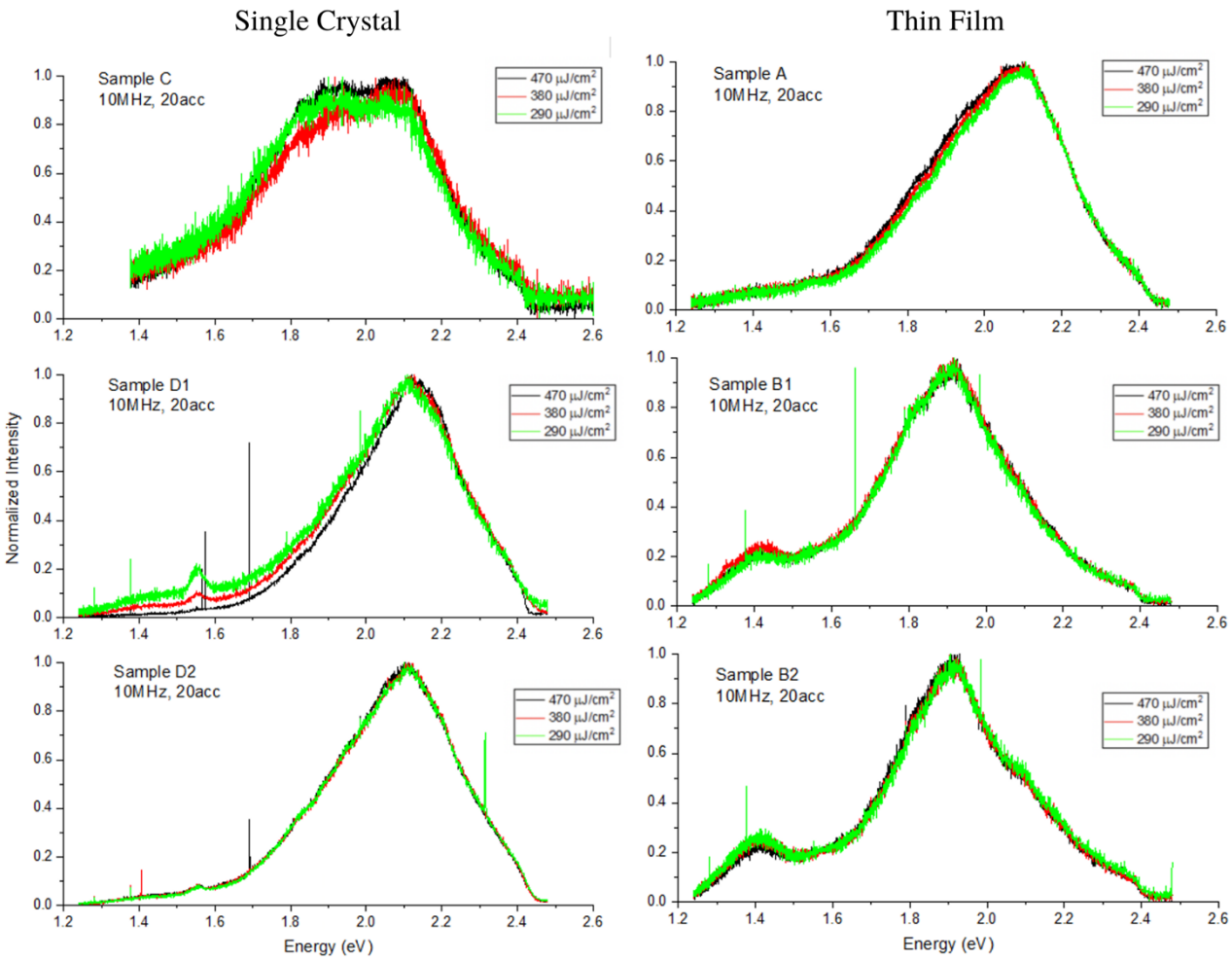


***Figure 36.*** *Single crystal (left) spectra collected from two samples, with two points on one sample, at three different fluences, compared with thin film (right) spectra collected from two samples, with two points on one sample, at three different fluences.*

The spectra on the left-hand side of the figure are from the single crystal samples, and the spectra on the right-hand side of the figure are from the thin film samples. Only thin film sample A's spectra shape resembles the shape of the spectra generated at two different points on single crystal sample D. These three spectra all exhibit peaks at 2.1 eV. Sample C also has a peak at 2.1 eV. Additionally, thin film samples B1 and B2 have a peak at 1.9 eV, which is where sample C's first peak is observed.

Similarly, we aimed to compare the decay characteristics between thin film and single crystal samples, as shown in Figure 37.

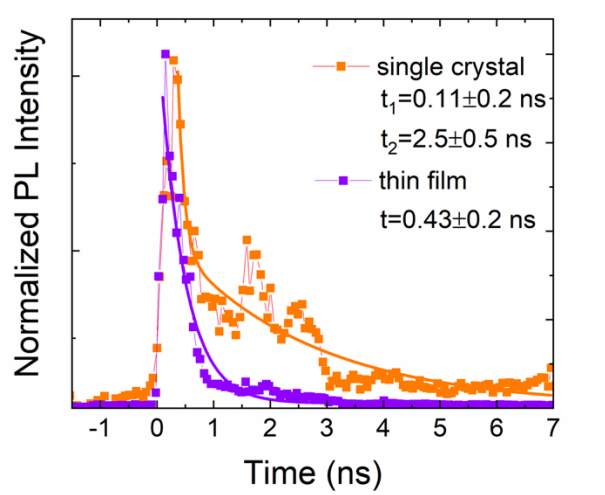


***Figure 37.*** *Radiative decay histograms showing normalized photoluminescence intensity versus time for both a single crystal sample (orange) and a thin film sample (purple) with decay fits and carrier lifetimes identified.*

While the thin film has a single exponential decay with ~ 0.35 ns, the thin film exhibits longer lifetime that can be described by a double exponential with the fast component ~ 0.25 ns and a much longer (1-2 ns) component. This results in a longer overall carrier lifetime in single crystalline samples.

We expanded upon this data by creating a side-by-side comparison of the decays for both single crystal and thin film samples. These are given in Figure 38. The thin film decays are depicted on the left-hand side of the figure, and the single crystal decays are depicted on the right-hand side.

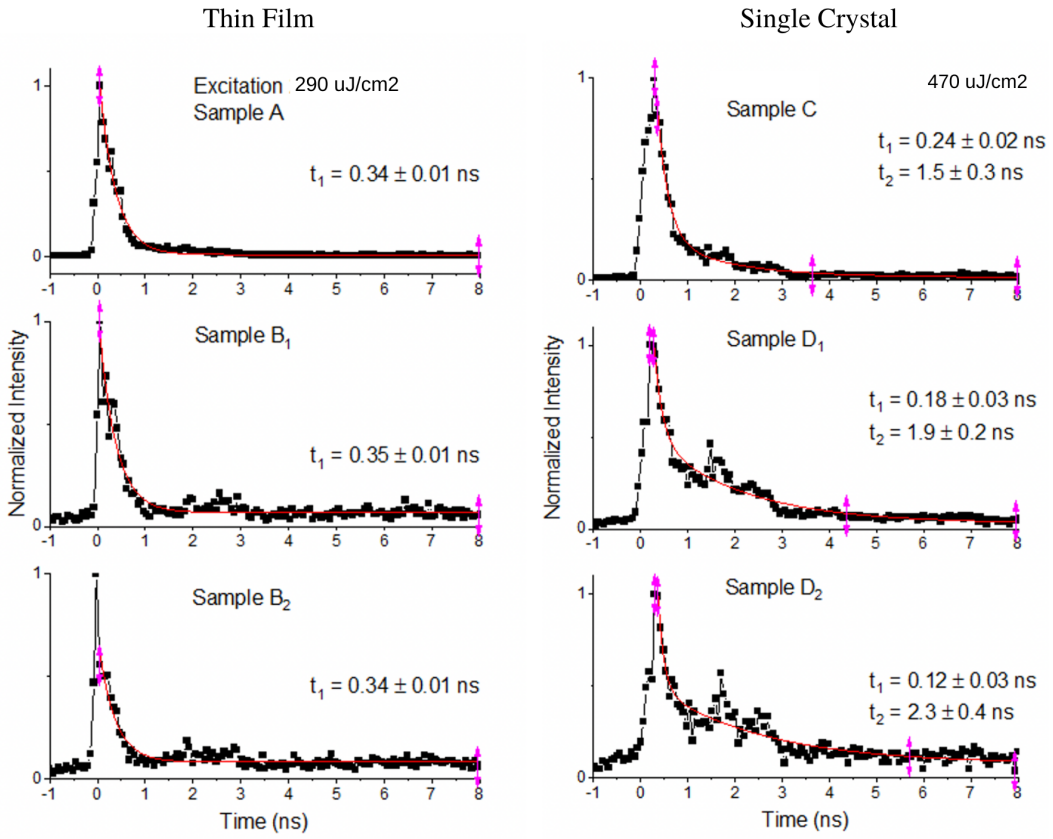


***Figure 38.*** *Radiative decay histograms showing normalized intensity versus time (ns) for thin film samples (left) and single crystal samples (right), with decay fits and carrier lifetimes included. Thin film samples were fit with ExpDec1 while single crystal sample were fit with ExpDec2.*

Here, we consistently observe the presence of a longer, bi-exponential decay in single crystal samples.

## IV. Discussion

In the results we obtained from our thin film samples, we observed peaks in the emission spectra that are higher than the expected band gap energy. Samples B1 and B2, which, upon visible inspection, had a more vibrant red color compared to sample A, (Figure 22), exhibited peak emissions closer to the band gap energy than sample A did (Figure 24). As excitation laser photon energy (2.56 eV) is significantly higher than the band gap, we hypothesize that above-gap emission with a lifetime ~ 0.35 ns could originate from the excitons bound to the higher-lying defect states. Similar effects have been previously observed in inorganic perovskites such as $CsPbCl_3$ and $CsPbBr_3$ (Sebastian et al., 2015). This observation suggests that the binding energy

of the excitons in $Cs_2TiBr_6$ is indeed high, but temperature-dependent optical measurements and theoretical calculations are needed to explore this idea further. The thin film data also exhibited a small peak at around 1.4 eV, which is likely attributed to defect state emission. For the single crystal samples, the emission is linear in excitation fluence. For the thin film sample, emission intensity shows saturation as available states fill.

Additionally, we observed that the decay time constants for all our thin film samples, as seen in Figure 26, were experimentally equivalent (~ 0.35 ns, well above experimental resolution of ~ 0.1 ns) after uncertainty was accounted for. This implies that the samples had a high degree of homogeneity in properties, both between different samples and within a single sample at different data points.

As seen in Figure 36, single crystal emission is narrower than that of a thin film, with the peak ~ 2.1 eV being most prominent. This observation is consistent with this peak, present in single crystal and thin film samples alike, originating from an exciton bound to a higher-lying bulk defect state. Its radiative lifetime is longer in the single crystal, suggesting that additional grain boundary states in the polycrystalline thin film act as non-radiative recombination centers.

We also found that PL emission of single crystals is strongly impacted by small cracks in the PL chamber, indicating that freshly cleaved surfaces rapidly oxidize in the presence of oxygen. When the sample is oxidized, lower energy peak at 1.9 eV becomes more prominent (Sample C, Figure 31). This might suggest that this emission is related to the oxide states. Alternatively, since this emission is closer to the observed band edge, surface oxidation reduces the number of the defect states that can serve as higher-energy exciton traps at ~ 2.1 eV. Future planned experiments using in-situ oxidation of the sample will provide additional information necessary to unambiguously assign the observed spectral features.

As expected, the thin film samples which likely have a much higher defect density have shorter radiative lifetimes than the single crystal samples. Longer carrier lifetimes are more ideal for solar panel/PV applications, suggesting that more work needs to be done to improve the thin film quality for realistic PV applications of $Cs_2TiBr_6$'s efficiencies.

## 1. Sustainability

Green technology is crucial for mitigating the climate crisis, but there are additional environmental implications and human rights violations associated with its creation. These issues

must be acknowledged before widespread implementation of this technology can occur. Development of green technologies often involves technological and material substitution to replace harmful components with less environmentally problematic ones. Such substitutions include the replacement of fossil fuel technologies with solar energy, as well as the replacement of silicon solar panels with perovskite cells. Before approaching these solutions, material sourcing, relative earth abundance, extraction, and toxicity must be researched. All technologies are likely to have harmful processes and practices associated with their creation and usage, but it's important to acknowledge these effects and work to minimize them as much as possible.

One of the more overlooked consequences of technological substitution is the effect it has on vulnerable populations. The critical minerals in high demand for use in green technologies are frequently sourced from vulnerable communities and ecosystems, leading to disruption of community dynamics, destruction of ecosystems and livelihoods, and exploitation of vulnerable populations. Additionally, the political environments of low-income countries often give way to exploitation by world economic powers. Some examples include the cobalt rush in the Democratic Republic of Congo, and bauxite mining in Guinea. The effects our developments have on these communities are not always visible to us, so they are regularly ignored despite their major ethical implications on technological substitution. Because of the uncertain nature of technology and advancement, these processes require carefully monitored infrastructure and governance. To support local communities where resources are being extracted, there needs to be sufficient consideration and reparations to ensure minimal damage and population displacement.

Based on the research outlined in the background of this report and the progress made experimentally in the results, $Cs_2TiBr_6$ is a material of significant interest for future solar panel production. This perovskite-like material is cheaper and faster to produce, using fewer resources and producing lower amounts of emissions during production and refinement than their widely used silicon counterparts. It simultaneously appeals economically to powerholders interested in making the switch to renewables. Additionally, life cycle assessments have shown that the more common lead-based perovskite alternatives have toxicity risks throughout the commodity chain. With titanium as a substitute, $Cs_2TiBr_6$ is safer for workers, users, and the environment throughout all phases of the solar panel's life cycle.

One specific concern about $Cs_2TiBr_6$ is its sourcing, particularly the cesium and titanium components. Cesium is relatively rare globally, sparking concerns about abundance and ability to

mine enough for widespread use in solar panels without depletion. Additionally, because the largest mines are currently monopolized by China, sourcing on the scale required for broader production would likely be expensive. Raw cesium is also highly reactive and must be handled with care throughout the production chain, requiring sufficient PPE and resources for workers. With China's history of colonial control and unregulated mining practices in the Democratic Republic of the Congo (DRC), as discussed in the background, there may be additional concerns about mining regulations and safety precautions. However, there are new potential mining sites in North America that would allow for easier access and greater regulation for safer extraction. With a push to upscale the mining operation for cesium, a heightened understanding of its implications on human rights and the environment must be pursued.

In contrast, titanium is a highly abundant metal. This makes it an effective alternative to other common perovskite base metals. It also lacks the major toxicity concerns of lead and tin, making it a seemingly ideal substitute. However, titanium production and fabrication processes can become costly due to the high reactivity of the metal with oxygen, nitrogen, and hydrogen in the air at elevated temperatures. These costly processes also have environmental consequences, such as destruction of ecosystems in mining areas and loss of topsoil. Additionally, the U.S. has a heavy reliance on imports of titanium, which can become costly and does not allow for sufficient regulation of mining processes. Despite this, there are also some domestic titanium sources, providing potential avenues for cost reduction and greater regulation. $Cs_2TiBr_6$ is not perfect, but there is a lot of potential for sustainable sourcing and upscaling. If efficiency issues are addressed through effective sealing processes to prevent degradation while still rivaling the output of traditional silicon solar panels, pursuing this new perovskite-like material alternative would be positive for the environment and public health while saving time and money during production. Perovskites can be created in short amounts of time and are cheap to grow. This perovskite-like material also lacks lead or other heavy metals, making it less ecologically damaging if it leaches under environmental stressors. This also ensures the safety of those who handle it during the production process. It is important to acknowledge the material's downfalls and how the technology's components are sourced when pursuing a sustainable future, but these externalities are not reasons to cease pursuit of implementation.

## 2. Future Work

In the future, additional research can be pursued on how the samples are sealed and observed. Gas sealing is a possible future project to explore. Through encapsulating samples with $TiO_2$, there is an opportunity to improve the stability of the material. If $Cs_2TiBr_6$ is going to be pursued as a possible PV material, it must also be exposed to other environmental conditions, such as controlled heat and moisture, while in the sealed cell to determine how it withstands other atmospheric situations. Additional data from thin film and single crystal samples could also be collected to better understand unexpected emission data and determine which form has more potential for industry usage.

In general, it is necessary to improve the quality of mines for workers, the environment, and surrounding communities. It is essential to address environmental issues related to proposed mining and give serious consideration to those whose rights and lands are being infringed upon. Studies should be conducted to determine possible adverse effects, with publicized results to allow for greater community understanding and involvement. Additionally, any displaced or harmed parties should be provided with sufficient reparations. In response to the desire to develop products with minimal overstepping of human rights, the Business and Human Rights Resource Center has developed the Transition Minerals Tracker, which allows companies to keep tabs on human rights allegations to ensure that materials are ethically sourced (Nogrady, 2020). Technology like this allows for improvements in material sourcing to better avoid human rights violations. Another important step towards a green energy transition is to collectively work towards equitable distribution of solar technologies between different races and class groups. Climate change cannot be effectively mitigated if solar energy becomes just another green technology that only caters to the wealthy. Determination of viable pathways to make solar energy accessible to all must be pursued, such as loans for solar panel installation and credit incentives.

# V. Conclusion

In this project, we used time-resolved photoluminescence (PL) spectroscopy to investigate the optical emission and carrier lifetime in both single crystal and thin-film $Cs_2TiBr_6$,

an emerging material for use in solar cells. We researched and collected data on the origins of prominent emission features of the material, as well as the dependence these features had on sample morphology and different environmental conditions. Additionally, we investigated the sustainability of the material's extraction and usage, bringing attention to the need for acknowledgement of sourcing and safety concerns.

Using photoluminescence spectroscopy (PL), we observed and collected data on optical properties of $Cs_2TiBr_6$ thin film and single crystal under dry nitrogen atmospheric conditions. We found than $Cs_2TiBr_6$ has an indirect bandgap of ~1.85 eV for thin film samples and 1.76 eV for single crystal samples, with closely positioned direct gap. Sealed crystals and films, protected from oxidation, were found to emit broadband photoluminescence following excitation with 485 nm laser. In both cases, emission was centered above the band gap, with the blue shift of emission relative to the gap being more pronounced in the bulk crystals. This observation leads us to hypothesize that the origin of the emission is excitons bound to high-lying bulk defect states. This emission is longer lived in single crystals as additional grain boundary defects may act as nonradiative recombination centers in the polycrystalline thin films.

Future work will be guided by the hypotheses developed in this thesis. Specifically, in-situ oxidation studies where oxygen will be slowly introduced into the sealed PL cell and PL spectra recorded continuously will determine the role of surface oxidation on spectra and carrier lifetimes. In addition, experiments where oxidized samples are etched to remove the oxide and re-examined in the PL setup will be helpful. To implement efficient PV devices, both stability and short carrier lifetime must be addressed. Sealing the surface of $Cs_2TiBr_6$ with protective $TiO_2$ layers might be an effective approach to improve stability, but the impact of $TiO_2$ on optical properties needs to be investigated as well. More data would also be helpful to determine the reasons more effectively for discrepancies in shapes between the various samples. Additional work on comparisons between oxidized and unoxidized samples could also be pursued to clarify our observations. Furthermore, there is a long way to go to make upscaling this material's use in solar panels more sustainable. The implications of resource extraction on environments in developing countries and on public health of all involved along the supply chain must be pursued before widespread implementation. This may involve sufficient PPE, reparations, and even just the general acknowledgement of the existence of these concerns.

# Works Cited


Abuodha, J. O. Z. (2002). Environmental Impact Assessment of the Proposed Titanium Mining Project in Kwale District, Kenya. *Marine Georesources & Geotechnology*, *20*(3), 199–207. https://doi.org/10.1080/03608860290051895

AfricaNews. (2021, September 9). *Coup puts spotlight on Guinea's huge bauxite reserves*. Africanews. https://www.africanews.com/2021/09/09/coup-puts-spotlight-on-guinea-s-huge-bauxite-reserves/

Babayigit, A., Ethirajan, A., Muller, M., & Conings, B. (2016). Toxicity of organometal halide perovskite solar cells. *Nature Materials*, *15*(3), 247–251. https://doi.org/10.1038/nmat4572

Bhattacharya, S., & John, S. (2019). Beyond 30% Conversion Efficiency in Silicon Solar Cells: A Numerical Demonstration. *Scientific Reports*, *9*(1), 12482. https://doi.org/10.1038/s41598-019-48981-w

Britt, J., & Ferekides, C. (1993). *Thin-film CdS/CdTe solar cell with 15.8% efficiency*. 3.

Business & Human Rights Resource Centre. (2017). Report claims titanium mining host community has not benefited from mining operations. https://www.business-humanrights.org/en/latest-news/report-claims-titanium-mining-host-community-has-not-benefited-from-mining-operations/

Cao, J., Wu, B., Chen, R., Wu, Y., Hui, Y., Mao, B.-W., & Zheng, N. (2018). Efficient, Hysteresis-Free, and Stable Perovskite Solar Cells with ZnO as Electron-Transport Layer: Effect of Surface Passivation. *Advanced Materials*, *30*(11), 1705596. https://doi.org/10.1002/adma.201705596

*Cesium*. (n.d.). Minerals Education Coalition. https://mineralseducationcoalition.org/minerals-database/cesium/

Chen, M., Ju, M.-G., Carl, A. D., Zong, Y., Grimm, R. L., Gu, J., Zeng, X. C., Zhou, Y., & Padture, N. P. (2018). Cesium Titanium(IV) Bromide Thin Films Based Stable Lead-free Perovskite Solar Cells. *Joule*, *2*(3), 558–570. https://doi.org/10.1016/j.joule.2018.01.009

Correa-Baena, J.-P., Saliba, M., Buonassisi, T., Gratzel, M., Abate, A., Tress, W., & Hagfeldt, A. (2017). Promises and challenges of perovskite solar cells. *Science*, *358*(6364), 739–744. DOI: 10.1126/science.aam6323

Danylenko, M. (2018, May 23). Photovoltaics: Materials Used and How Their Efficiency and Cost Can Be Improved. *Materials and Engineering Resources - Matmatch.* https://matmatch.com/resources/blog/solar-panels-materials-efficiency-cost/

De los Reyes, G. (2015). *Ultrafast Photoluminescence Spectroscopy of Silicon Nanocrystals*. University of Alberta.

De Rooij, D. (n.d.). Silicon (Si) for solar cells: How is it produced? https://sinovoltaics.com/learning-center/solar-cells/silicon-si-solar-cells-produced/

Dirjish, M. (2012, May 16). *What's The Difference Between Thin-Film And Crystalline-Silicon Solar Panels?* Electronic Design. https://www.electronicdesign.com/technologies/power-sources/article/21796492/whatsthe-difference-between-thinfilm-and-crystallinesilicon-solar-panels

Entner, R. (n.d.). *2.3 Carrier Generation and Recombination*. https://www.iue.tuwien.ac.at/phd/entner/node11.html

Espinosa, N., Serrano-Luján, L., Urbina, A., & Krebs, F. C. (2015). Solution and vapor deposited lead perovskite solar cells: Ecotoxicity from a life cycle assessment

perspective. *Solar Energy Materials and Solar Cells*, *137*, 303–310. https://doi.org/10.1016/j.solmat.2015.02.013

Euvrard, J., Wang, X., Li, T., Yan, Y., & Mitzi, D. B. (2020). Is Cs2TiBr6 a promising Pb-free perovskite for solar energy applications? *Journal of Materials Chemistry A*, *8*(7), 4049–4054. https://doi.org/10.1039/C9TA13870F

Fitzgerald, P. (n.d.). *Spatially Resolved Photoluminescence Spectroscopy of 2D Nanomaterials*. Worcester Polytechnic Institute.

Fox, M. (2001). *Optical Properties of Solids*. Oxford University Press.

Gearino, D. (2020, June 11). Inside Clean Energy: The Racial Inequity in Clean Energy and How to Fight It. *Inside Climate News*. https://insideclimatenews.org/news/11062020/inside-clean-energy-racial-inequity-solar/

Geoscience Australia. (2018, March 4). *Titanium* https://www.ga.gov.au/education/classroom-resources/minerals-energy/australian-mineral-facts/titanium

Graedel, T. E. (2002). Material substitution: A resource supply perspective. *Resources, Conservation and Recycling*, *34*(2), 107–115. https://doi.org/10.1016/S0921-3449(01)00097-0

*Grain Boundary (GB)*. (2020). Corrosionpedia. http://www.corrosionpedia.com/definition/599/grain-boundary-gb

HORIBA. (n.d.). *What is Photoluminescence spectroscopy?* https://www.horiba.com/en_en/products/by-technique/molecularspectroscopy/photoluminescence-pl-electroluminescence-el/

Jarosz, G., Marczyński, R., & Signerski, R. (2020). Effect of band gap on power conversion

efficiency of single-junction semiconductor photovoltaic cells under white light phosphor-based LED illumination. *Materials Science in Semiconductor Processing*, *107*, 104812. https://doi.org/10.1016/j.mssp.2019.104812

Ju, M.-G., Chen, M., Zhou, Y., Dai, J., Ma, L., Padture, N. P., & Zeng, X. C. (2018). Toward Eco-friendly and Stable Perovskite Materials for Photovoltaics. *Joule*, *2*(7), 1231–1241. https://doi.org/10.1016/j.joule.2018.04.026

Kwak, J. I., Nam, S.-H., Kim, L., & An, Y.-J. (2020). Potential environmental risk of solar cells: Current knowledge and future challenges. *Journal of Hazardous Materials*, *392*, 122297. https://doi.org/10.1016/j.jhazmat.2020.122297

Leuenberger, A., Winkler, M. S., Cambaco, O., Cossa, H., Kihwele, F., Lyatuu, I., Zabré, H. R., Farnham, A., Macete, E., & Munguambe, K. (2021). Health impacts of industrial mining on surrounding communities: Local perspectives from three sub-Saharan African countries. *PLOS ONE*, *16*(6), e0252433. https://doi.org/10.1371/journal.pone.0252433

Levenda, A. M., Behrsin, I., & Disano, F. (2021). Renewable energy for whom? A global systematic review of the environmental justice implications of renewable energy technologies. *Energy Research & Social Science*, *71*, 101837. https://doi.org/10.1016/j.erss.2020.101837

Luo, S., Dauod, W. A., Mater, J., (2014). Recent progress in organic-inorganic halide perovskite solar cells: mechanisms and materials design. *Journal of Materials Chemistry A.* 3. 10.1039/C4TA04953E

Makuła, P., Pacia, M., & Macyk, W. (2018). How To Correctly Determine the Band Gap Energy of Modified Semiconductor Photocatalysts Based on UV–Vis Spectra. *Th*

*Journal of Physical Chemistry Letters*, *9*(23), 6814-6817. https://doi.org/10.1021/acs.jpclett.8b02892

Marsh, J. (2020, June 21). Perovskite Solar Cells: What You Need To Know | EnergySage. *Solar News*. https://69.88.159.222/perovskite-solar-cells/

McCluskey, M., & Janotti, A. (2020). Defects in Semiconductors: Journal of Applied Physics: Vol 127, No 19. *Journal of Applied Physics*, *127*(19). https://doi.org/10.1063/5.0012677

McGill University. (n.d.). What is sustainability? https://www.mcgill.ca/sustainability/files/sustainability/what-is-sustainability.pdf

Mendes, J. L., Gao, W., Martin, J. L., Carl, A. D., Deskins, N. A., Granados-Focil, S., & Grimm, R. L. (2020). Interfacial States, Energetics, and Atmospheric Stability of Large-Grain Antifluorite Cs2TiBr6. *The Journal of Physical Chemistry C*, *124*(44), 24289–24297. https://doi.org/10.1021/acs.jpcc.0c08719

Metcalfe, T. (2021). *Solar panels are reaching their limit. These crystals could change that.* https://www.nbcnews.com/science/environment/solar-panels-are-reaching-limit-crystals-change-rcna545

National Renewable Energy Laboratory. (2021). New Perovskite Design Shows Path to Higher Efficiency. https://www.nrel.gov/news/program/2021/new-perovskite-design-shows-path-to-higherefficiency.html

Niarchos, N. (2021, May 24). *The Dark Side of Congo's Cobalt Rush | The New Yorker*. https://www.newyorker.com/magazine/2021/05/31/the-dark-side-of-congos-cobalt-rush

Nogrady, B. (2020, May 14). Cobalt is critical to the renewable energy transition. How can we minimize its social and environmental cost? *Ensia*. https://ensia.com/features/cobalt-sustainability-batteries/

Nover, J., Zapf-Gottwick, R., Feifel, C., Koch, M., Metzger, J. W., & Werner, J. H. (2017). Long-term leaching of photovoltaic modules. *Japanese Journal of Applied Physics*, *56*(8S2), 08MD02. https://doi.org/10.7567/JJAP.56.08MD02

Office of Energy Efficiency and Renewable Energy. (n.d.). *Perovskite Solar Cells*. Energy.Gov. https://www.energy.gov/eere/solar/perovskite-solar-cells

OilPrice.com. (2020). *Cesium Wars: Is America Ready To Challenge China Over This Critical Metal*. PR Newswire. https://www.prnewswire.com/news-releases/cesium-wars-is-america-ready-to-challenge-china-over-this-critical-metal-301006367.html

Osborne, M. (2016, February 23). First Solar pushes CdTe cell efficiency to record 22.1%. *PV Tech*. https://www.pv-tech.org/first-solar-pushes-cdte-cell-efficiency-to-record-22-1/

Peleg, R. (2018). *Duke team develops a method to create hybrid thin-film materials | Perovskite-Info*. https://www.perovskite-info.com/duke-team-develops-method-create-hybrid-thin-film-materials

Penn State Department of Energy and Mineral Engineering. (n.d.). *4.1 Photovoltaic effect | EME 812: Utility Solar Power and Concentration*. https://www.eeducation.psu.edu/eme812/node/534

Potter, K. S., & Simmons, J. H. (2021). Chapter 5—Optical properties of semiconductors. In K. S. Potter & J. H. Simmons (Eds.), *Optical Materials (Second Edition)* (pp. 229–307). Elsevier. https://doi.org/10.1016/B978-0-12-818642-8.00005-3

Ramos-Ruiz, A., Wilkening, J. V., Field, J. A., & Sierra-Alvarez, R. (2017). Leaching of cadmium and tellurium from cadmium telluride (CdTe) thin-film solar panels under

simulated landfill conditions. *Journal of Hazardous Materials*, *336*, 57–64. https://doi.org/10.1016/j.jhazmat.2017.04.052

Ranjan, S., Balaji, S., Panella, R. A., & Ydstie, B. E. (2011). Silicon solar cell production. *Computers & Chemical Engineering*, *35*(8), 1439–1453. https://doi.org/10.1016/j.compchemeng.2011.04.017

RENEW. (n.d.). *Renewable Energy Worcester*. Co-Op Power. https://www.cooppower.coop/worcester

Rong, Y., Hu, Y., Mei, A., Tan, H., Saidaminov, M., Seok, S., McGehee, M., Sargent, E., & Han, H. (2018). Challenges for commercializing perovskite solar cells. *Science*, *361*(6408). https://www.science.org/doi/10.1126/science.aat8235

Saha-Dasgupta, T. (2020). Double perovskites with 3d and 4d/5d transition metals: Compounds with promises. *Materials Research Express*, *7*(1), 014003. https://doi.org/10.1088/2053-1591/ab6293

Saki, Z., Byranvand, M. M., Taghavinia, N., Kedia, M., & Saliba, M. (2021). Solution-processed perovskite thin-films: The journey from lab- to large-scale solar cells. *Energy & Environmental Science*, *14*(11), 5690–5722. https://doi.org/10.1039/D1EE02018H

Saliba, M., Matsui, T., Seo, J.-Y., Domanski, K., Correa-Baena, J.-P., Khaja Nazeeruddin, M., M. Zakeeruddin, S., Tress, W., Abate, A., Hagfeldt, A., & Grätzel, M. (2016). Cesium-containing triple cation perovskite solar cells: Improved stability, reproducibility and high efficiency. *Energy & Environmental Science*, *9*(6), 1989–1997. https://doi.org/10.1039/C5EE03874J

Schileo, G., & Grancini, G. (2021). Lead or no lead? Availability, toxicity, sustainability and environmental impact of lead-free perovskite solar cells. *Journal of Materials Chemistry*

*C*, *9*(1), 67–76. https://doi.org/10.1039/D0TC04552G

Schultz, L. (2020). *How the transition to renewable energy can include climate justice*. Wisconsin Energy Institute. https://energy.wisc.edu/news/how-transition-renewable-energy-can-include-climatejustice

Seagle, S. (n.d.). *Titanium processing | Technology, Methods, & Facts*. Britannica. https://www.britannica.com/technology/titanium-processing

Shi, Z., & Jayatissa, A. H. (2018). Perovskites-Based Solar Cells: A Review of Recent Progress, Materials and Processing Methods. *Materials*, *11*(5), 729. https://doi.org/10.3390/ma11050729

*Silicosis*. (n.d.). NORD (National Organization for Rare Disorders). https://rarediseases.org/gard-rare-disease/silicosis/

Skocaj, M., Filipic, M., Petkovic, J., & Novak, S. (2011). Titanium dioxide in our everyday life; is it safe? *Radiology and Oncology*, *45*(4), 227–247. https://doi.org/10.2478/v10019-011-0037-0

Tilton, J. E. (1991). Material substitution: The role of new technology. *Technological Forecasting and Social Change*, *39*(1), 127–144. https://doi.org/10.1016/0040-1625(91)90032-B

Tom, J. (2021, June 30). *UV-Vis Spectroscopy: Principle, Strengths and Limitations and Applications*. Analysis & Separations from Technology Networks. https://www.technologynetworks.com/analysis/articles/uv-vis-spectroscopy-principle-strengths-and-limitations-and-applications-349865

Trueman, D. (2021, October 13). *Cesium, A Critical Metal and an Opportunity for Avalon*

*Advanced Materials*. InvestorIntel. https://investorintel.com/markets/technology-metals/technology-metals-intel/cesium-a-critical-metal-and-an-opportunity-for-avalon-advanced-materials/

Tsoutsos, T., Frantzeskaki, N., & Gekas, V. (2005). Environmental impacts from the solar energy technologies. *Energy Policy*, *33*(3), 289–296. https://doi.org/10.1016/S0301-4215(03)00241-6

*Types of recombination*. PVEducation. (n.d.). https://www.pveducation.org/pvcdrom/pnjunctions/typesofrecombination#footnote1_xtf3p6j

UCLA. (n.d.). What is Sustainability? UCLA Sustainability. https://www.sustain.ucla.edu/what-is-sustainability/

Union of Concerned Scientists. (2013). *Environmental Impacts of Solar Power*. https://www.ucsusa.org/resources/environmental-impacts-solar-power

United Nations. (n.d.). Sustainability. United Nations; United Nations. https://www.un.org/en/academic-impact/sustainability

Universität Basel. (2013, August 2). *Cobalt replacements make solar cells more sustainable*. ScienceDaily. https://www.sciencedaily.com/releases/2013/08/130802080232.htm

US EIA. (2021). *Frequently Asked Questions (FAQs)—U.S. Energy Information Administration (EIA)*. https://www.eia.gov/tools/faqs/faq.php

US EIA. (n.d.). *U.S. Price of Natural Gas Delivered to Residential Consumers (Dollars per Thousand Cubic Feet)*. https://www.eia.gov/dnav/ng/hist/n3010us3m.htm

US EPA (2014, November 5). Learn About Sustainability [Overviews and Factsheets]. https://www.epa.gov/sustainability/learn-about-sustainability

Vij, P., & Hardej, D. (2012). Evaluation of tellurium toxicity in transformed and non-transformed human colon cells. *Environmental Toxicology and Pharmacology*, *34*(3), 768–782. https://doi.org/10.1016/j.etap.2012.09.009

Virginia Energy. (n.d.). *Titanium*. https://energy.virginia.gov/geology/Titanium.shtml

Watts, J., Kirk, A., McIntyre, N., Gutiérrez, P., & Kommenda, N. (2021). *Half world's fossil fuel assets could become worthless by 2036 in net zero transition*. The Guardian. https://www.theguardian.com/environment/ng-interactive/2021/nov/04/fossil-fuel-assets-worthless-2036-net-zero-transition

Williams, A. (2019, December 19). What's An Exciton? *Hackaday*. https://hackaday.com/2019/12/19/whats-an-exciton/

Woodhouse, M., Feldman, D., Fu, R., Horowitz, K., & Chung, D. (2016). *On the Path to SunShot: The Role of Advancements in Solar Photovoltaic Efficiency, Reliability, and Costs*. 44.

Wormington, J. (2018). *"What Do We Get Out of It?": The Human Rights Impact of Bauxite Mining in Guinea*. Human Rights Watch. https://www.hrw.org/report/2018/10/04/what-do-we-get-out-it/human-rights-impact-bauxite-mining-guinea

Ye, R., & Barron, A. (n.d.). *Photoluminescence Spectroscopy and its Applications—Physical Methods in Chemistry and Nano Science—OpenStax CNX*. https://cnx.org/contents/uieDnVBC@25.2:gbsDEZju@2/PhotoluminescenceSpectroscopy-and-its-Applications

# Appendices

## Appendix A – Procedure for Crystal Synthesis

*Part 1 – Preparing*

1. Take a 1in diameter clear quartz tube (length varies) and clean it with 1 part hydrogen peroxide and 3 parts sulfuric acid. Rinse with water and place in an oven until completely dry.
2. Measure out about 1.100g of CsBr, place in a clean vial and leave in the oven to drive off all the water.
3. Once everything is dry, they get placed in the glovebox.
4. In the glovebox about 1.500g of $TiBr_4$ is measured out. A funnel (either the length of the quartz tube or longer) is carefully placed inside the quartz tube (careful to not touch the walls of the quartz tube to avoid contamination and facets growing on the sides of the tube). The reactants are then added through the funnel.
5. The funnel is carefully removed, and a butterfly valve is then secured to the open-ended side of the tube. The butterfly valve prevents air from getting in the tube during transfer.
6. The quartz tube is then removed from the glovebox without tipping or shaking the reactants.
7. We then attach the top of the butterfly valve to the Schlenk line inside one of our fume hoods. The tube is pumped down and a motor is turned on so that the quartz tube starts to rotate at a consistent speed. A torch is then held against the top of the tube to seal it off and close both sides.

*Part 2 - Heating*

8. It is then left to cool for a couple minutes and afterwards it is placed in one of our lab furnaces, elevated by a piece of fiber quartz so that the reactants don't move from the bottom end of the tube.
9. Jocelyn Mendez's heating recipe is then followed. It's entered like this in one of our computers connected to the Titan furnace.

| Front (°C) | Back (°C) | Time (Hours) |
|---|---|---|
| Ramp up to 680 | Ramp up to 710 | 15 |
| Go/hold it at 680 | Go/hold at 710 | 24 |
| Ramp down to 450 | Ramp down to 470 | 15 |
| Ramp down to 220 | Ramp down to 240 | 15 |
| Ramp down to 0 | Ramp down to | 15 |

*Part 3 – Obtaining*

10. Once it's done the quartz tube is placed in a plastic bag and is pumped into the glovebox with a wrench.
11. With the plastic bag closed the quartz tube is carefully broken up with the wrench, the crystal facets are separated from the glass slowly and carefully and placed in a vial.

*Part 4 – Sealing*

12. In the glovebox a facet is chosen from the vial and cleaved with a clean razor blade.
13. It is then placed on a quartz round held by an aluminum plate, a gasket is placed around the crystal facet and then another aluminum plate and quartz round are placed on top.
14. 6 screws are carefully placed in their designated holes securing the two aluminum plates in place. Everything is tightened and it's then ready for data collection.